OFFICE OF NAVAL RESEARCH
Contract N00014-77-C-0236
Task No. NR 356-639

TECHNICAL REPORT NO. 1

A RHEOLOGICAL AND OPTICAL PROPERTIES INVESTIGATION OF ALIPHATIC (NYLON-66, PγBLG) AND AROMATIC (KEVLAR®, NOMEX®) POLYAMIDE SOLUTIONS

by

Hiroshi Aoki
James L. White
John F. Fellers

Prepared for Publication
in the
Journal of Applied Polymer Science

Polymer Engineering
The University of Tennessee
Knoxville, Tennessee 37916

January 13, 1978

SECURITY CLASSIFICATION OF THIS PAGE (When Data Entered)

REPORT DOCUMENTATION PAGE

READ INSTRUCTIONS BEFORE COMPLETING FORM

1. REPORT NUMBER: 1	2. GOVT ACCESSION NO.
3. RECIPIENT'S CATALOG NUMBER	
4. TITLE (and Subtitle): A RHEOLOGICAL AND OPTICAL PROPERTIES INVESTIGATION OF ALIPHATIC (NYLON-66, PγBLG) AND AROMATIC (KEVLAR®, NOMEX®) POLYAMIDE SOLUTIONS	5. TYPE OF REPORT & PERIOD COVERED: 4-1-77 thru Technical 1-13-78
	6. PERFORMING ORG. REPORT NUMBER: PSE Report No. 107
7. AUTHOR(s): Hiroshi Aoki, James L. White, and John F. Fellers	8. CONTRACT OR GRANT NUMBER(s): N00014-77-C-0236
9. PERFORMING ORGANIZATION NAME AND ADDRESS: Polymer Engineering, The University of Tennessee, Knoxville, TN 37916	10. PROGRAM ELEMENT, PROJECT, TASK AREA & WORK UNIT NUMBERS
11. CONTROLLING OFFICE NAME AND ADDRESS: Office of Naval Research, 800 N. Quincy Street, Arlington, VA 22217	12. REPORT DATE: 1-13-78 13. NUMBER OF PAGES: 42
14. MONITORING AGENCY NAME & ADDRESS (if different from Controlling Office): ONR Resident Representative, U. of Alabama Research Institute, P.O. Box 1247, Huntsville, AL 35807	15. SECURITY CLASS. (of this report) 15a. DECLASSIFICATION/DOWNGRADING SCHEDULE

16. DISTRIBUTION STATEMENT (of this Report)

Approved for Public Release; Distribution Unlimited.

17. DISTRIBUTION STATEMENT (of the abstract entered in Block 20, if different from Report)

18. SUPPLEMENTARY NOTES

To be published in the Journal of Applied Polymer Science

19. KEY WORDS (Continue on reverse side if necessary and identify by block number)

Polyamides, Aromatic, Aliphatic, Solutions, Liquid Crystals, Rheological Properties, Optical Properties

20. ABSTRACT (Continue on reverse side if necessary and identify by block number)

An experimental study of shear viscosity $\eta(\dot{\gamma})$, principal normal stress difference N_1 $(\dot{\gamma})$, storage modulus $G'(\omega)$, dynamic viscosity $\eta'(\omega)$ and filament elongation to break L_B is reported for solutions of several polyamides; namely, (Nylon-66), poly (γ-Benzyl-L-Glutamate), (Nomex®) and (Kevlar®). The variation of properties with concentration, aliphatic vs aromatic polymer and solvent type is emphasized. The

DD FORM 1 JAN 73 1473 EDITION OF 1 NOV 65 IS OBSOLETE

S/N 0102-LF-014-6601

SECURITY CLASSIFICATION OF THIS PAGE (When Data Entered)

importance of forming liquid crystalline phases in Kevlar® and PγBLG solutions on such properties is indicated.

SYNOPSIS

An experimental study of shear viscosity $\eta(\dot{\gamma})$, principal normal stress difference N_1 $(\dot{\gamma})$, storage modulus $G'(\omega)$, dynamic viscosity $\eta'(\omega)$ and filament elongation to break L_B is reported for solutions of several polyamides; namely, (Nylon-66), poly(γ-Benzyl-L-Glutamate), (Nomex®) and (Kevlar®). The variation of properties with concentration, aliphatic vs aromatic polymer and solvent type is emphasized. The importance of forming liquid crystalline phases in Kevlar® and PγBLG solutions on such properties is indicated.

INTRODUCTION

The solution properties of polyamides have gained scientific attention as a result of the recently reported aromatic structures and their commercial importance (1-6).

Poly (Hexamethylene Adipamide), Nylon-66, and Poly (Caprolactam), Nylon-6, have been important commercial polymers for almost forty years. More recently aromatic polyamides, notably Nomex® and Kevlar® fiber, have become important (1). While aliphatic polyamides are fusible and processed in the molten state to form fibers and molded parts, aromatic polyamides chemically degrade below their melting temperature and must be processed in the solution state. This has led to an increased interest in the solution properties of polyamides. Studies of aromatic polyamide solutions have turned up a number of striking experimental observations. Concentrated solutions of p-linked aromatic polyamides exhibit liquid crystalline behavior (1-5), while solutions of m-linked ones show complex effects with salts in solution plus association (6-7). The liquid crystalline behavior is similar to that observed in concentrated solutions of polypeptides (8-12).

The present authors and their coworkers have been concerned with the processing and properties of polyamides (13), structure development in the melt (14-16) and wet (16-17) spinning of nylon-6 and nylon-66 fibers as well as wet spinning Nomex® and Kevlar® fibers (17). In related papers, new types of aromatic polyamides were synthesized and solution spun into fibers (18-19).

In this paper, we investigate the rheological and optical properties of four polyamides of varying structure. Up to the present most such investigations were limited to the shear viscosity, however we also consider normal stresses, sinusoidal oscillation response and apparent spinnability.

We give our greatest attention to comparing aliphatic, m-linked and p-linked polyamides formed from diamines and dicarboxylic acids, specifically

Poly(hexamethylene adipamide) (Nylon-66)

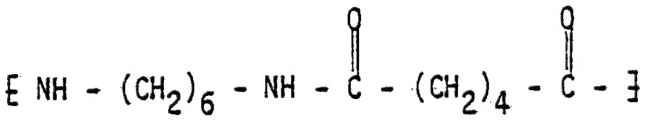

(I)*

Poly(m-phenylene isophthalamide) (Nomex®)

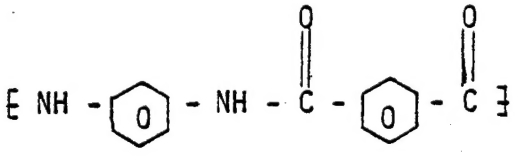

(II)

Poly(p-phenylene terephthalamide) (Kevlar®)

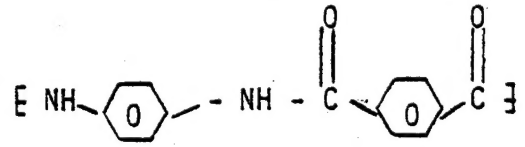

(III)

We also studied a polypeptide previously reported in the literature as liquid crystalline (8-12),

Poly(γ-benzyl-L-glutamate) (PγBLG)

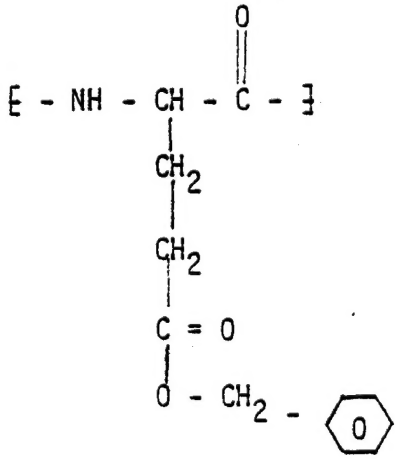

(IV)

---

*The symbols I, II, III, IV are maintained on all figures.

The rheological properties and possible onset of liquid crystalline character are studied in different solvents. In the case of polymers (I), (II), and (III), we contrast their properties in H_2SO_4. In a sense, this paper specifically continues research described in two earlier papers. The polymer-solvent systems wet spun by Hancock, Spruiell, and White (17) are included in the systems described here. The physico-chemical properties including rheological and optical behavior of poly(m-phenylene isophthalamide) (II) in dimethylacetamide/LiCl solvents have been investigated by Aoki, Harwood, Lee, Fellers and White (7) and we shall report here on some of its characteristics in H_2SO_4 as well.

EXPERIMENTAL

Materials

Four polymers with structures indicated in I thru IV above have been investigated in our studies. Their characteristics are summarized in Table I. Polymer I, poly(hexamethylene adipamide) was a DuPont Zytel® molding resin. Polymer II, Poly(m-phenylene isophthalamide) was a DuPont Nomex® (type 430) synthetic fiber, Polymer III was DuPont Kevlar® synthetic fiber. Polymer IV was a PγBLG purchased from Sigma Chemical Company, Saint Louis, Missouri.

The solvents used in this study were 100% sulfuric acid (H_2SO_4) obtained from Fisher Scientific Company, Fair Lawn, New Jersey, Dimethylacetamide (DMA) obtained from Aldrich Chemical Company, Milwakee, Wisconsin, lithium chloride (LiCl) from Fisher Scientific Company, and m-cresol from Aldrich Chemical Company.

The polymer solvent combinations studied were

I - 100% H_2SO_4, 90% $HCOOH/H_2O$

II - 100% H_2SO_4, DMA with 5% LiCl

III - 100% H_2SO_4

IV - m-Cresol

Optical Measurements

Each polymer-solvent system was studied in a light microscope between cross polarizer and analyzer. Specifically the Kwolek DDA test was carried out (1). Samples of polymer solution were placed between two glass slides separated from each other by Teflon tape, of thickness 0.165 mm. The increase in $I/_{Io}$, the amount of light passing through the system with polymer solution present, was measured as a function of polymer concentration by means of a light meter.

Rheological Measurements

Steady shear flow and sinusoidal oscillation experiments were carried out in a Model R16 Weissenberg Rheogoniometer. A special Type 304 stainless steel cone-plate apparatus was designed and built in our shops for the H_2SO_4 experiments. It was checked and calibrated against the standard aluminum cone-plate with a non-corrosive polymer solution. This cone-plate fixture has an angle α of 2^o and a radius R of 5 cm.

In a steady shear flow, the shear rate in a cone-plate geometry is

$$\dot{\gamma} = \Omega \alpha \qquad (1)$$

The stress response involves a shear stress σ_{12} and three normal stresses σ_{11}, σ_{22}, and σ_{33}; where (1) is the direction of flow, (2) the direction of shear and (3) the neutral direction. The normal stresses are generally

represented through an isotropic pressure p and two normal stress differences N_1 and N_2 defined as

$$N_1 = \sigma_{11} - \sigma_{22} \tag{2a}$$

$$N_2 = \sigma_{22} - \sigma_{33}$$

Three rheological functions are defined by relating N_1, N_2, and σ_{12} to shear rate through the expressions

$$\sigma_{12} = \eta\dot{\gamma}^2 \tag{3a}$$

$$N_1 = \psi_1\dot{\gamma}^2 \tag{3b}$$

$$N_2 = \psi_2\dot{\gamma}^2 \tag{3c}$$

Here η is the viscosity and ψ_1 and ψ_2 are normal stress coefficients.

Determination of σ_{12} and N_1 were calculated from rheogoniometer torque, T, and vertical thrust, F, measurements. This was carried out using the expressions (20)

$$\sigma_{12} = \frac{3T}{2\pi R^3} \tag{4a}$$

$$N_1 = \frac{2F}{\pi R^2} \tag{4b}$$

In the oscillartory shear flow a sinusoidal strain $\gamma(t)$ is imparted to the fluid between the cone and plate. We may express this as

$$\gamma_{12}(t) = \gamma_0 \sin\omega t \tag{5}$$

where ω is the frequency and γ_0 the shear strain amplitude. The shear stress response is out of phase with the strain. It may be represented as

$$\sigma_{12} = G'(\omega)\,\gamma_0 \sin\omega t + G''(\omega)\,\gamma_0 \cos\omega t \tag{6a}$$

$$= G'(\omega)\,\gamma(t) + \eta'(\omega)\,\frac{d\gamma}{dt}$$

Where $G'(\omega)$ is the dynamic storage modulus, $G''(\omega)$ is the loss modulus and $\eta'(\omega)$ is the dynamic viscosity. In phase and out of phase stress components were obtained using Eq(6a) and converted to $G'(\omega)$ and $\eta'(\omega)$.

Spinnability Experiments

An apparatus was designed to estimate the spinnability of polymer solutions. Its principle and design are summarized in Figure 1. A rod is initially in contact with the surface of a polymer solution. It is withdrawn at velocity V inducing a cylindrical liquid filament of length L, equal to Vt, where t is the time elapsed to form the filament between the surface of the liquid and the moving member. The existence of the filament is measured by electrical conduction. When the filament breaks at length L, the contact is broken. The apparatus is similar to an instrument described by Sherr (21) more than a generation old.

OPTICAL STUDIES

Results

Measurements of transmitted polarized light $I/_{Io}$ in the Kwolek DDA test are shown as a function of concentration for the polymers studied in Figure 2. At low concentrations, essentially no light is transmitted. At high concentrations, the solutions of polymers III and IV transmit significant quantities of light while the other solutions do not. The transition occurs at concentrations of 9.5% for the Kevlar® and at 9% for the PγBLG.

Interpretation

The dilute solutions of all polymers studied are optically isotropic in a state of rest. However, optical anisotropy arises in solutions of Kevlar® and PγBLG. Such anisotropy may be due to stress induced birefringence (22-23) or to liquid crystalline character (1-5, 8-13). If it is due to the former, it should decay with time in a solution until it disappears. However, if the solution is a soft gel rather than a true fluid, such birefringence could be permanent.

The two polymer solutions found to transmit polarized light have both been reported as liquid crystalline by earlier investigators. The solutions of Kevlar® are reported as such by DuPont investigators (1, 2). PγBLG solutions are a classical case of liquid crystalline behavior in polymers (8-12).

VISCOSITY STUDIES

Results

Plots of viscosity η as a function of shear rate $\dot{\gamma}$ are shown for the solutions of Nylon-66 at 25°C in Figure 3, Nomex® at 25°C in Figure 4 and Kevlar® at 25°C in Figure 5 and at 60°C in Figure 6. It is clear that solvent quality has a strong influence on viscosity in these systems. At any concentration the H_2SO_4 solution data are the highest for both Nylon-66 and Nomex®. Kevlar® is only soluble in H_2SO_4.

The general behavior of the viscosity-shear rate-concentration relationship for solutions of Polymers I, II, and III differ. In the case of Nylon-66 and Nomex®, the response is Newtonian at low shear rates with $\eta(\dot{\gamma})$ decreasing with shear rates at large $\dot{\gamma}$ at the higher concentrations studied. For Kevlar® at 25°C (Figure 5) the response is qualitatively

different. The viscosity does not exhibit Newtonian behavior even at the lowest shear rates and the data continue to increase with a slope of 45^{o} on logarithmic paper. Furthermore the viscosity in this system, especially at high shear, does not increase monotonically with concentration. Instead, the viscosity strikes a maximum and then decreases at high concentration.

Figure 6 shows the response of the same system at 60^{o}C. The regular low shear rate response is no longer found and the solutions are close to Newtonian. However, the viscosity-concentration dependence still exhibits a maximum.

The viscosity-shear rate behavior of PγBLG in m-cresol is contained in Figure 7. The PγBLG possesses a Newtonian character similar to the Nylon-66 solutions but the viscosity-concentration dependence clearly exhibits a maximum.

Interpretation

Certain aspects of the experimental results require expanded consideration. First we note the unusual $n(\dot{\gamma})$ behavior of the concentration Kevlar®/H_2SO_4 solutions at 25^{o}C. This type of response has been found in other polymer systems, usually in polymer melts or solutions containing particulate fibers (24-26). It is considered to mean the material exhibits a yield value. This is illustrated in Figure 8 where we plot viscosity as a function of shear stress σ_{12}. It can be seen that the viscosity tends to infinity at a finite non-zero shear stress. This implies that there will be no flow in these systems below a critical shear stress of 700 dynes/cm^2. The Kevlar®/H_2SO_4 becomes a gel. It is possible that the system is however a fluid rather than a gel. Only the shear rates were not lowered far enough.

The viscosity-concentration behavior of the Kevlar® and PγBLG solutions deserve special attention as they exhibit a maximum at intermediate concentrations. This is shown in Figure 9 for Kevlar® at 25°C (at $\dot{\gamma}$ = 0.1 and 5.0 sec^{-1}) Kevlar® at 60°C and the PγBLG. We also include Nomex® in H_2SO_4 for comparison. The Kevlar® and PγBLG solutions show viscosity maxima. Shear rate concentration dependence of η is to a large extent influenced by the existence of a yield value at high shear stresses. The position of the viscosity maxima in PγBLG solutions has been previously noted by Hermans (10) and in p-linked aromatic polyamides by Kwolek and her coworkers (1-2) and by Papkov et al (3). It has been associated with the formation of liquid crystalline regions in these solutions and generally occurs at about the same concentration as the rise in transmitted light $I/_{Io}$ described in the previous section.

It is of interest to the above considerations that similar viscosity decreases have been found associated with the formation of nematic liquid crystalline phases in low molecular weight organic compounds (27). These organic compounds exist as isotropic liquids at high temperatures and solid crystals at low temperatures. In an intermediate temperature range, they behave as nematic liquid crystals. It was found by Porter and Johnson (27), that in the isotropic liquid state the viscosity increases as temperature decreases as would be expected in normal liquids. However, when the transition temperature to the liquid crystalline state is reached, there was a substantial drop in viscosity.

The principal normal stress difference coefficient ψ_1 for the Polymer I through IV systems is plotted as a function of shear rate $\dot{\gamma}$ in figures 10 to 13. The magnitude of normal stresses varies considerably with solvent for

any particular polymer and with polymer type. For the Nylon-66 and Nomex® systems the H_2SO_4 solutions have higher normal stresses. The Kevlar® ψ_1 data are generally higher than those of Nomex® and Nylon-66 but seem to exhibit a maximum with respect to concentration. The normal stresses in PγBLG solutions are quite small and can only be observed at the highest concentrations. Generally the normal stress coefficient is a decreasing function of shear rate and tends to become constant at low shear rates.

The dependence of ψ_1 in Kevlar® solutions on shear rate, shear stress and concentration is of special interest. In Figure 12 we see at low shear rates the ψ_1 values for 10 and 12 percent solutions are significantly larger than those of 6 and 8 percent solutions, but decreased rapidly with shear rate. This is to be compared with the viscosity-shear rate behavior of the same concentration. In Figure 14 we plot ψ_1 as a function of σ_{12}. This seems consistent with the idea of a yield value in the more concentrated solutions. Figure 15 plots ψ_1 as a function of concentration evaluated a 0.5 and 5 SEC $^{-1}$ for 25°C at 5 SEC $^{-1}$ for 60°C. Maxima are observed at both temperatures.

OSCILLATORY EXPERIMENTS

Results

This experimental investigation was not as extensive as the shear flow studies. Figures 16 to 18 show typical plots of $G'(\omega)$ and $\eta'(\omega)$ as functions of frequency and concentration. The data of Figure 16 are for Nylon-66, Figure 17 for Nomex® solutions, and Figure 18 is for Kevlar® in H_2SO_4 at 25°C and 60°C. The curves of the latter at 25°C are rather different from the former with $\eta'(\omega)$ becoming indefinitely larger at low frequency and $G'(\omega)$ having a finite rather than zero asymptote.

Interpretation

The experimental data of Figure 16 and 17 are very typical of isotropic viscoelastic fluids. Generally in comparing the dynamic viscosity $\eta'(\omega)$ and the steady shear viscosity $\eta(\dot{\gamma})$ one has

$$\lim_{\omega \to 0} \eta'(\omega) = \lim_{\dot{\gamma} \to 0} \eta(\dot{\gamma}) = \eta_0 \tag{7a}$$

and

$$\eta(\dot{\gamma}) > \eta'(\omega = \dot{\gamma}) \tag{7b}$$

Similar experimental results have been reported for other concentrated polymer solutions.

The behavior of the Kevlar® solutions is similar at low concentrations. At high concentrations the response changes considerably. At low ω , $\eta'(\omega)$ increases indefinitely as ω decreases and

$$\eta(\dot{\gamma}) < \eta'(\omega = \dot{\gamma}) \tag{8}$$

for Kevlar® at 25°C. The shape of the G' (ω) curves are different from those of Figure 18 for the Nylon-66, Nylon-6 and Nomex®.

Consider

$$\tan \delta = \frac{G''(\omega)}{G'(\omega)} = \frac{\omega \eta'(\omega)}{G'(\omega)} \tag{9}$$

which represents the ratio of dissipated to stored energy (23). The 10 and 12 percent Kevlar® solutions at 25°C have a much lower value of tan δ at any frequency than the other soltions in this study. This indicates a more elastic solid like response.

We suggest the different linear viscoelastic characteristics of the 25°C Kevlar solutions is associated with the existence of the Gel structure dissussed in connection with our observations of the viscosity function $\eta(\dot{\gamma})$.

SPINNABILITY

Results

Figures 19 to 21 plot filament length to break L_b as a function of instron crosshead velocity for the various solutions investigated at 25°C. It is seen that the thread length which we interpret as spinnability varies considerably with polymer and solvent type. For the Nylon-66, the H_2SO_4 solutions have greater L_b than the HCOOH solutions. With the exception of the Kevlar®, L_b increases with concentration. Comparison at 8 percent concentration shows an ordering

Kevlar® > Nomex® > Nylon 66

in H_2SO_4.

Interpretation

The experiment reported here is similar to that analyzed by Ide and White (28, 29) except the elongation rate

$$E = \frac{V}{L(t)} \qquad (13)$$

decreases with time rather than being constant. However, the same mechanisms of failure - capillarity, ductile failure, and cohesive fracture occur and should interact similarly. From our observations, the dominant failure made appears to be capillarity at low concentrations and cohesive fracture at high concentrations.

It is of interest to compare the experimental observations made here with the wet spinning spinnability observations of Hancock and his coworkers (17). These authors found for any particular system that spinnability increases with concentration. We observed a similar variation of L_b. At

higher extension rates, both Kevlar® /H_2SO_4 and Nylon-66/H_2SO_4 show decreasing L_b. This may be due to high elongational viscosity induced brittle fracture. This type of phenomenon is predicted by Ide and White. At the same concentration Kevlar shows good spinnability among the polymers studied here, with the spinnability order being: Kevlar > Nomex > N-66.

ACKNOWLEDGEMENTS

This research was supported in part by Unitika Ltd. This work was supported in part by the Office of Naval Research.

TABLE I

Polymers Used in This Study

Polymer Designation	Polymer Type	Supplier	Molecular Weight $\times 10^{-3}$
I	Nylon 66	du Pont	28.4[a]
II	Nomex	du Pont	89[a]
III	Kevlar	du Pont	~40[b]
IV	PγBLG	Sigma Chemical	150[c]

(a) As reported in (16).
(b) As computed from (30).
(c) As reported by Sigma Chemical.

REFERENCES

1. Kwolek, S. L., U. S. Patent 3,671,542 (1972).

2. Kwolek, S. L., P. W. Morgan, J. R. Schaefgen and L. W. Gulrich, ACS Polymer Preprints, 17, 1153 (1974).

3. Papkov, S. P., V. G. Kulichikin, V. P. Kalmykova and A. Y. Malkin J. Poly. Sci., Polymer Phys., 17, 1169 (1974).

4. Wong, C. P., H. Ohnuma and G. C. Berry, ACS Polymer Preprints, 18, No. 1, 167 (1977).

5. White, J. L. and J. F. Fellers in "Fiber Structure and Properties" edited by J. L. White, Appl. Polymer Symp. (in press).

6. Klenin, V. I., L. V. Prozorov, M. Yu Prozorova and B. I. Zhizdyuk, J. Polym. Sci., C 44, 93 (1974).

7. Aoki, H., D. Harwood, Y. Lee, J. F. Fellers, and J. L. White, J. Appl. Polym. Sci., (submitted for publication).

8. Robinson, C., Trans. Faraday Soc., 52, 571 (1956).

9. Robinson, C., Tetrhedron, 13, 219 (1961).

10. Hermans, J., J. Colloid Sci., 17, 638 (1962).

11. Robinson, C., Mol. Crystals, 1, 467 (1966).

12. Samulski, E. T. and A. V. Tobolsky in "Liquid and Plastic Crystals," edited by G. W. Gray and P. Winsor, Wiley, NY (1974).

13. Aoki, H., D. R. Coffin, T. Hancock, D. Harwood, R. S. Lenk, J. F. Fellers and J. L. White in J. Polym. Sci., C (edited by C. Sroog and G. Berry) (in press).

14. Bankar, V. G., J. E. Spruiell and J. L. White, J. Appl. Polym. Sci., 21, 2341 (1977).

15. Danford, M., J. E. Spruiell, and J. L. White, J. Appl. Polym. Sci. (in press).

16. White, J. L. and J. E. Spruiell in "Fiber Structure and Properties," edited by J. L. White, Appl. Poly. Symp. (in press).

17. Hancock, T. A., J. E. Spruiell and J. L. White, J. Appl. Polym. Sci., 21, 1227 (1977).

18. Lenk, R. S., J. L. White and J. F. Fellers, J. Appl. Polym. Sci., 21, 1543, (1977).

19. Lenk, R. S., J. F. Fellers and J. L. White, Polymer J., 9, 9 (1977).

20. Middleman, S. "The Flow of High Polymers," Wiley, NY (1967).

21. Sherr, P. C., Rayon Textile Monthly, p. 67, (Feb.), (1945).

22. Treloar, L. R. G., "Physics of Rubber Elasticity," 2nd ed., Oxford (1958).

23. Tobolsky, A. B., "Properties and Structure of Polymers" Wiley, NY (1960).

24. Minagawa, W. and J. L. White, J. Appl. Polym Sci., 20, 501 (1976).

25. Vinogradov, G. V., A. Y. Malkin, E. P. Plotnikova, O. Y. Sabsal, and N. E. Nikolayeva in, J. Polym. Mat., 2, 1 (1972).

26. S. Onogi, Y. Mikami, and T. Matsumoto, Polym. Eng. Sci., 17, 1 (1977).

27. Porter, R. S. and J. F. Johnson, J. Appl. Phys., 34, 51 (1963).

28. Ide, Y. and J. L. White, J. Appl. Polym. Sci., 20, 2511 (1976).

29. Ide, Y. and J. L. White, J. Non-Newtonian Fluid Mech., 2, 281 (1977).

30. Tsvetkov, V. N. et al, European Polym. J., 13 455 (1977).

FIGURES

1. Spinnability Apparatus

2. Transmitted light I/Io as a function of polymer concentration for Polymers I-IV at 25°C.

3. Plot of viscosity $\eta(\dot{\gamma})$ as a function of shear rate $\dot{\gamma}$ for I, Poly(Hexamethylene Adipamide), in H_2SO_4 and 90% HCOOH at 25°C.

4. Plot of viscosity $\eta(\dot{\gamma})$ as a function of shear rate $\dot{\gamma}$ for II, Nomex®, in H_2SO_4 and Dimethylacetamide/5% LiCl at 25°C.

5. Plot of viscosity $\eta(\dot{\gamma})$ as a function of shear rate $\dot{\gamma}$ for III, Kevlar®, in H_2SO_4 at 25°C.

6. Plot of viscosity $\eta(\dot{\gamma})$ as a function of shear rate $\dot{\gamma}$ for III, Kevlar®, in H_2SO_4 at 60°C.

7. Plot of viscosity $\eta(\dot{\gamma})$ as a function of shear rate $\dot{\gamma}$ for IV, PγBLG, in m-cresol at 25°C.

8. Plot of viscosity η for Kevlar®/H_2SO_4 at 25°C as a function of shear stress σ_{12}.

9. Viscosity as a function of concentration for Kevlar®/H_2SO_4 at 25°C (0.1 and 4.0 SEC^{-1}), Kevlar®/H_2SO_4 at 60°C, PγBLG/m-cresol and Nomex®/H_2SO_4 at 25°C.

10. Principal normal stress difference coefficient $\psi_1(\dot{\gamma})$ as a function of shear rate and concentration for Nylon-66 in H_2SO_4 and HCOOH/10% H_2O at 25°C.

11. Principal normal stress difference coefficient $\psi_1(\dot{\gamma})$ as a function of shear rate and concentration for Nomex® in H_2SO_4 and DMA/5% LiCl at 25°C.

12. Principal normal stress difference coefficient $\psi_1(\dot{\gamma})$ as a function of shear rate and concentration for Kevlar®/H_2SO_4 at 25°C and 60°C.

13. Principal normal stress difference coefficient $\psi_1(\dot{\gamma})$ as a function of shear rate and concentration for PγBLG in m-cresol at 25°C.

14. Principal normal stress difference coefficient plotted as a function of shear stress σ_{12} for Kevlar®/H_2SO_4 solutions at 25°C.

15. Principal normal stress difference coefficient as a function of concentration for 25°C and 60°C Kevlar® /H_2SO_4 solutions.

16a. $G'(\omega)_0$ as a function of frequency for Nylon-66 solutions in HCOOH/10%H_2O at 25°C.

b. $\eta'(\omega)_0$ as a function of frequency for Nylon-66 solutions in HCOOH/10%H_2O at 25°C.

17a. $G'(\omega)$ as a function of frequency for Nomex® solutions at 25°C.

b. $\eta'(\omega)$ as a function of frequency for Nomex® solutions at 25°C.

18a. $G'(\omega)$ as a function of frequency for Kevlar® in H_2SO_4 at 25°C and 60°C.

b. $\eta'(\omega)$ as a function of frequency for Kevlar® in H_2SO_4 at 25°C and 60°C.

19. Length of threads to break for the Nylon-66 in H_2SO_4 and HCOOH spinnability experiments as a function of moving member speed and concentration at 25°C.

20. Length of threads to break for the Kevlar® /H_2SO_4 as a function of moving member speed and concentration at 25°C.

21. Comparison of length to break for Nylon-66, Nomex® and Kevlar® 8% solutions.

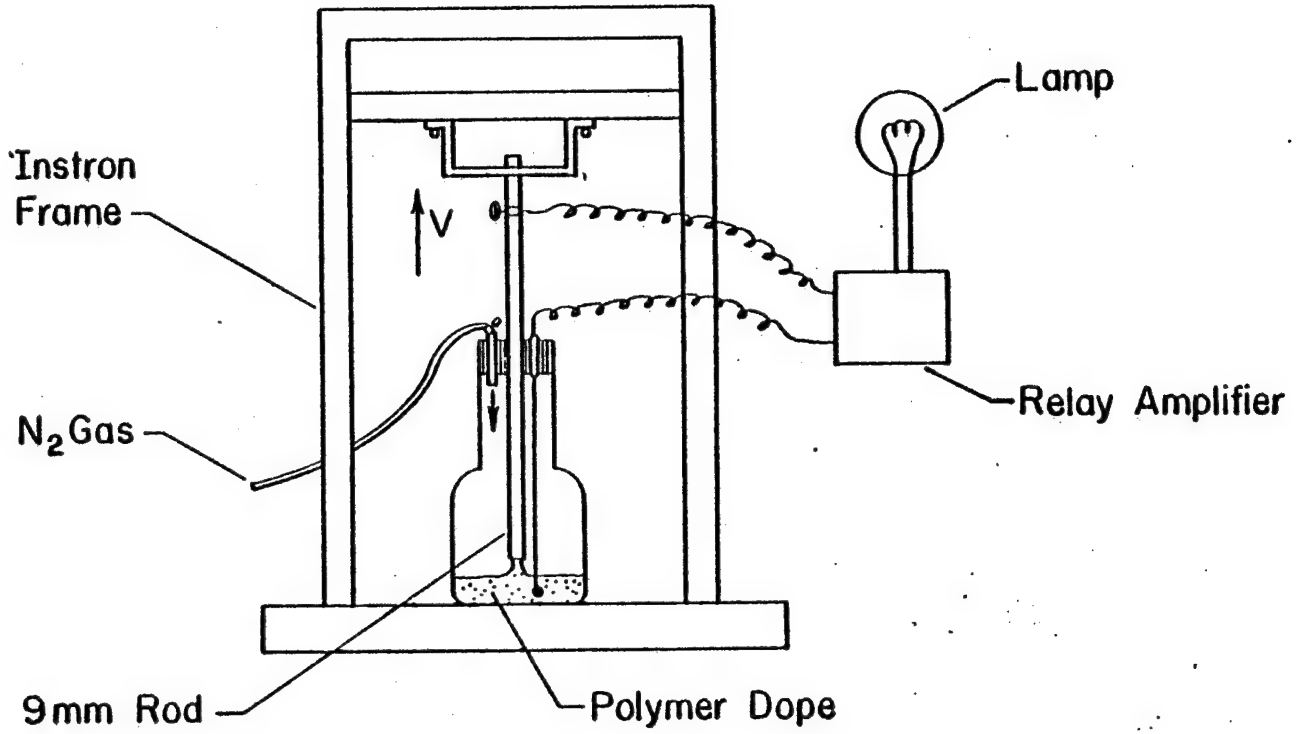

FIGURE 1. Spinnability Apparatus.

FIGURE 2. Transmitted light I/Io as a function of polymer concentration for Polymers I-IV at 25°C.

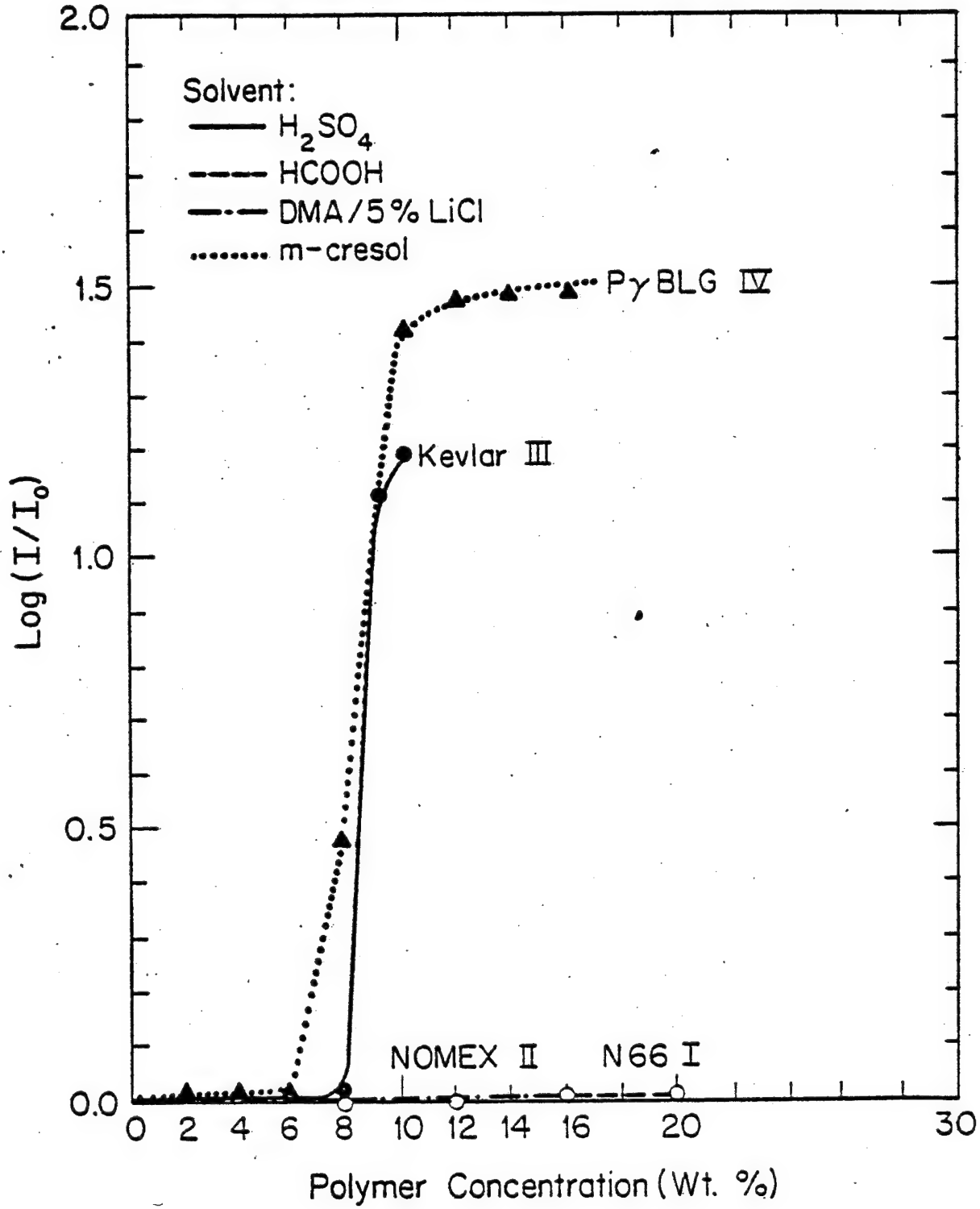

FIGURE 3. Plot of viscosity $\eta(\dot{\gamma})$ as a function of shear rate $\dot{\gamma}$ for I. Poly(Hexamethylene Adipamide), in H_2SO_4 and 90% HCOOH at 25°C.

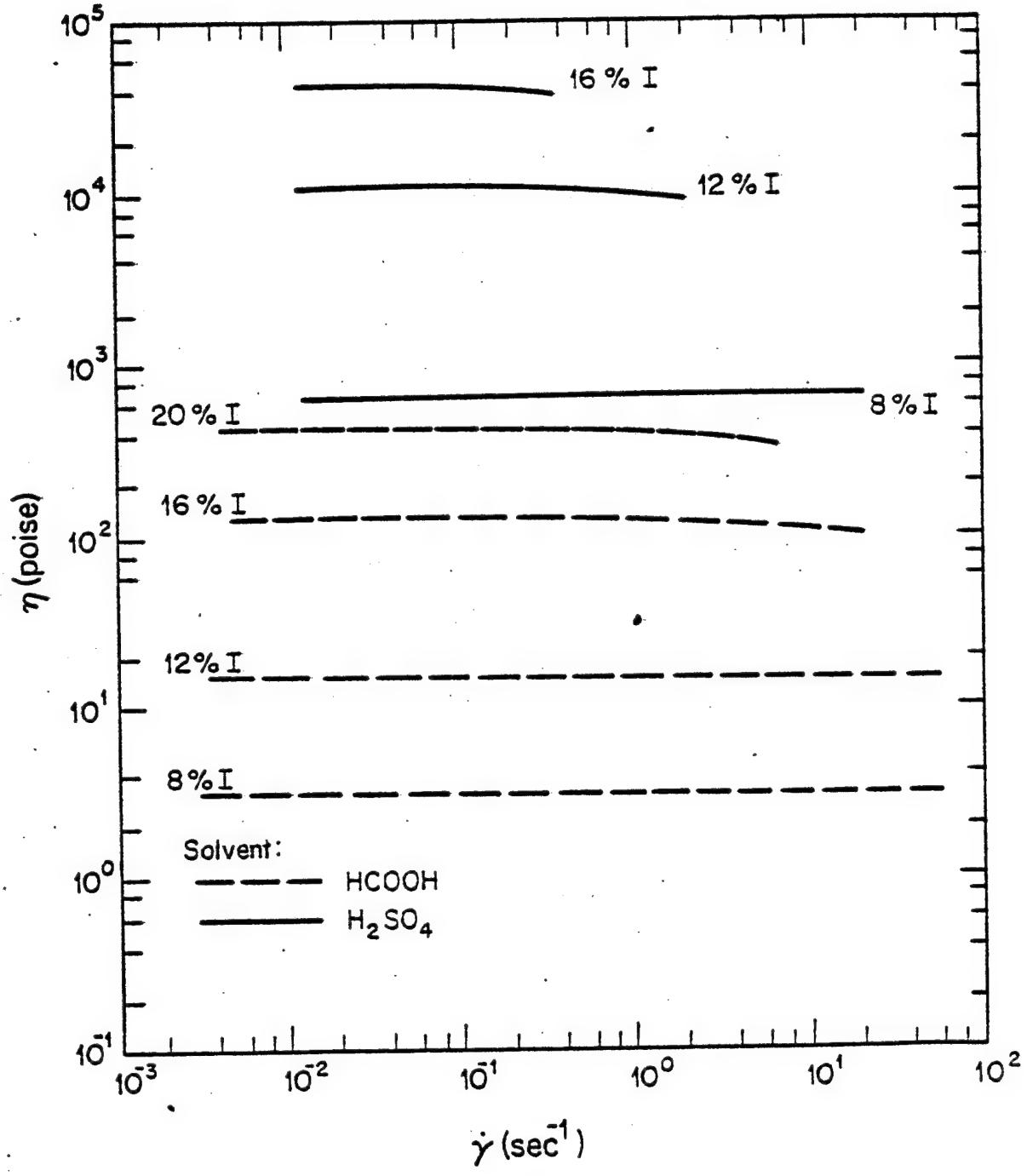

FIGURE 4. Plot of viscosity $\eta(\dot{\gamma})$ as a function of shear rate $\dot{\gamma}$ for II, Nomex®, in H_2SO_4 and Dimethylacetamide/5% LiCl at 25°C.

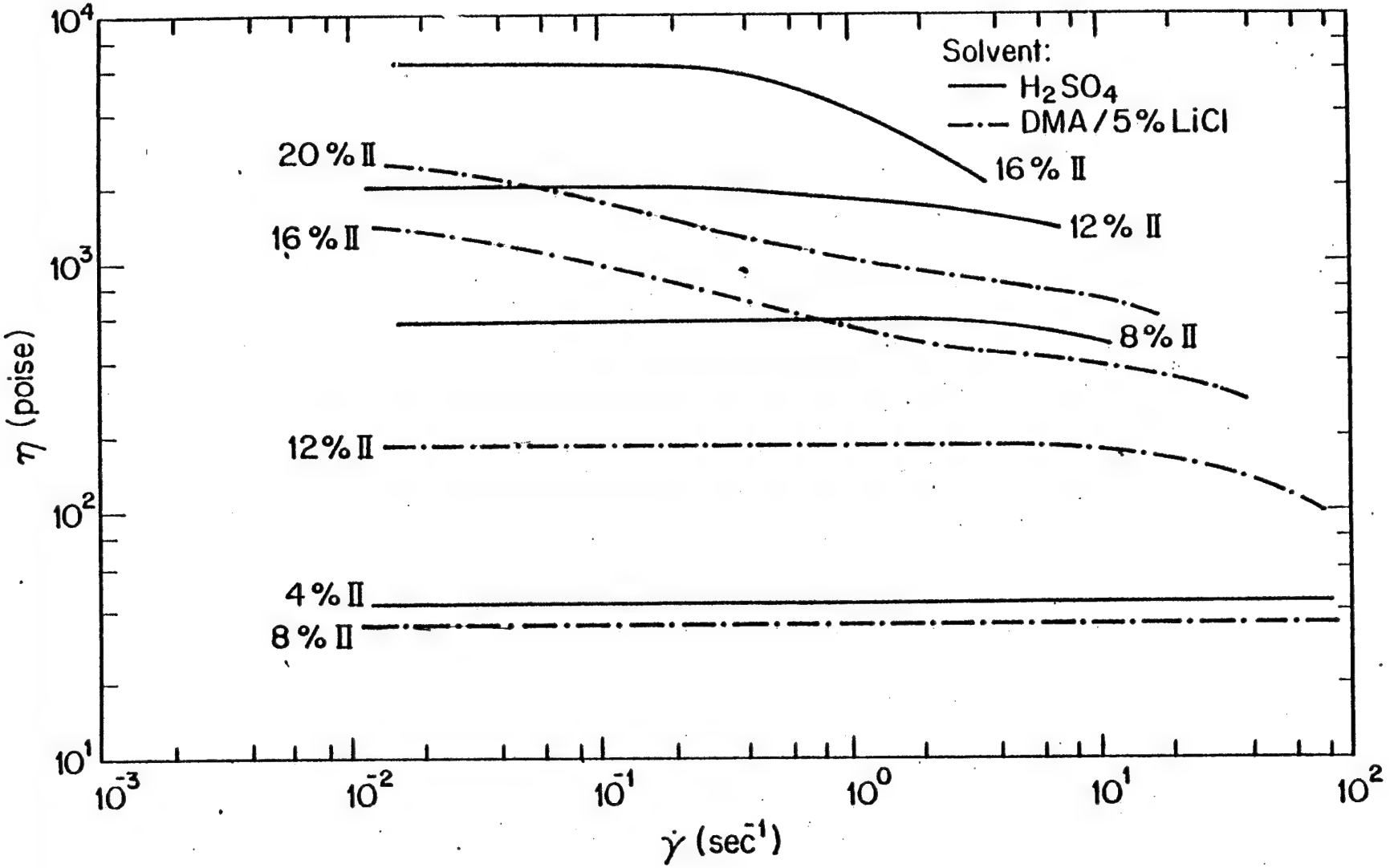

FIGURE 5. Plot of viscosity $\eta(\dot{\gamma})$ as a function of shear rate $\dot{\gamma}$ for III, Kevlar®, in H_2SO_4 at 25°C.

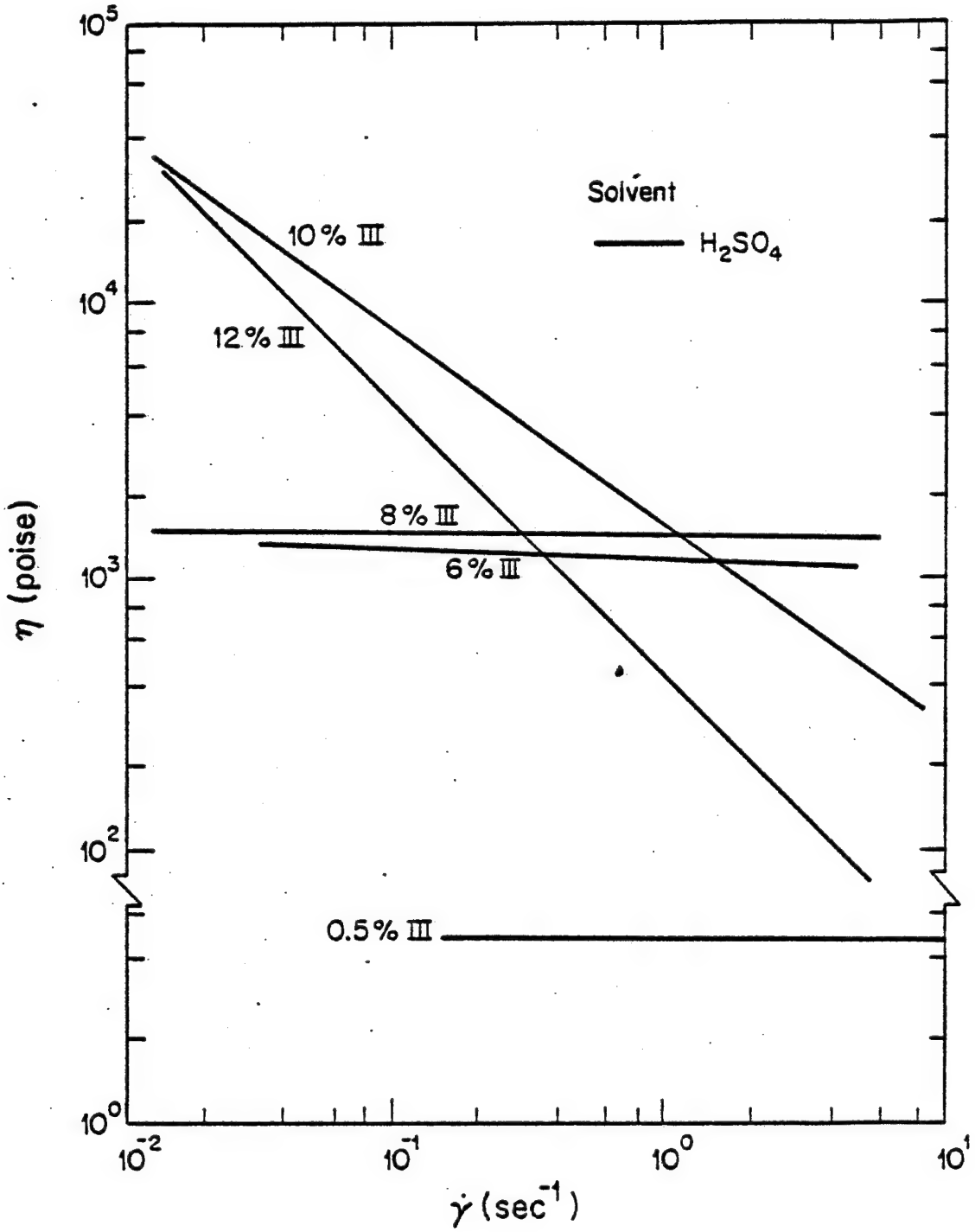

FIGURE 6. Plot of viscosity $\eta(\dot{\gamma})$ as a function of shear rate $\dot{\gamma}$ for III, Kevlar®, in H_2SO_4 at 60°C.

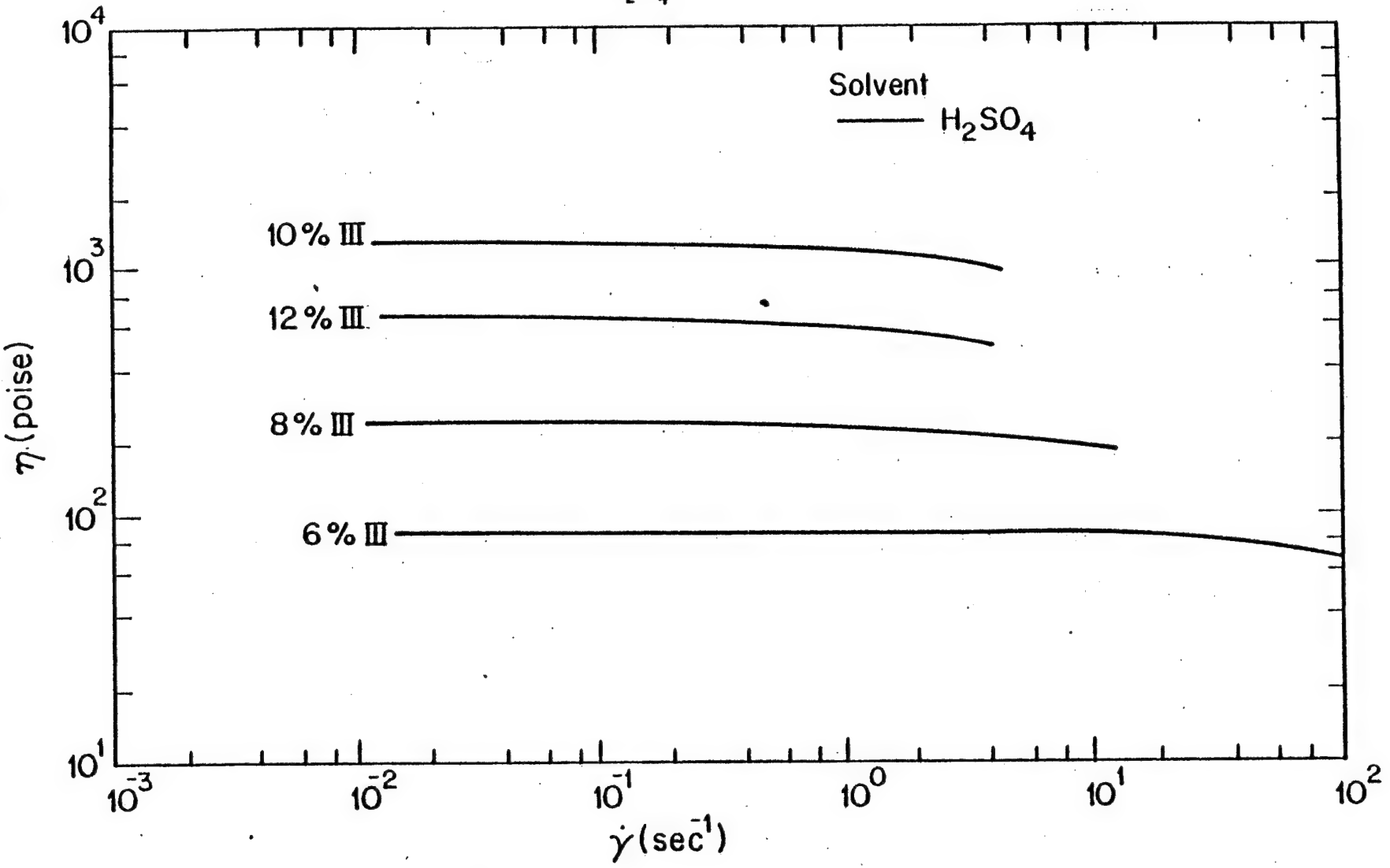

FIGURE 7. Plot of viscosity $\eta(\dot{\gamma})$ as a function of shear rate $\dot{\gamma}$ for IV, $P\gamma BLG$, in m-cresol at 25°C.

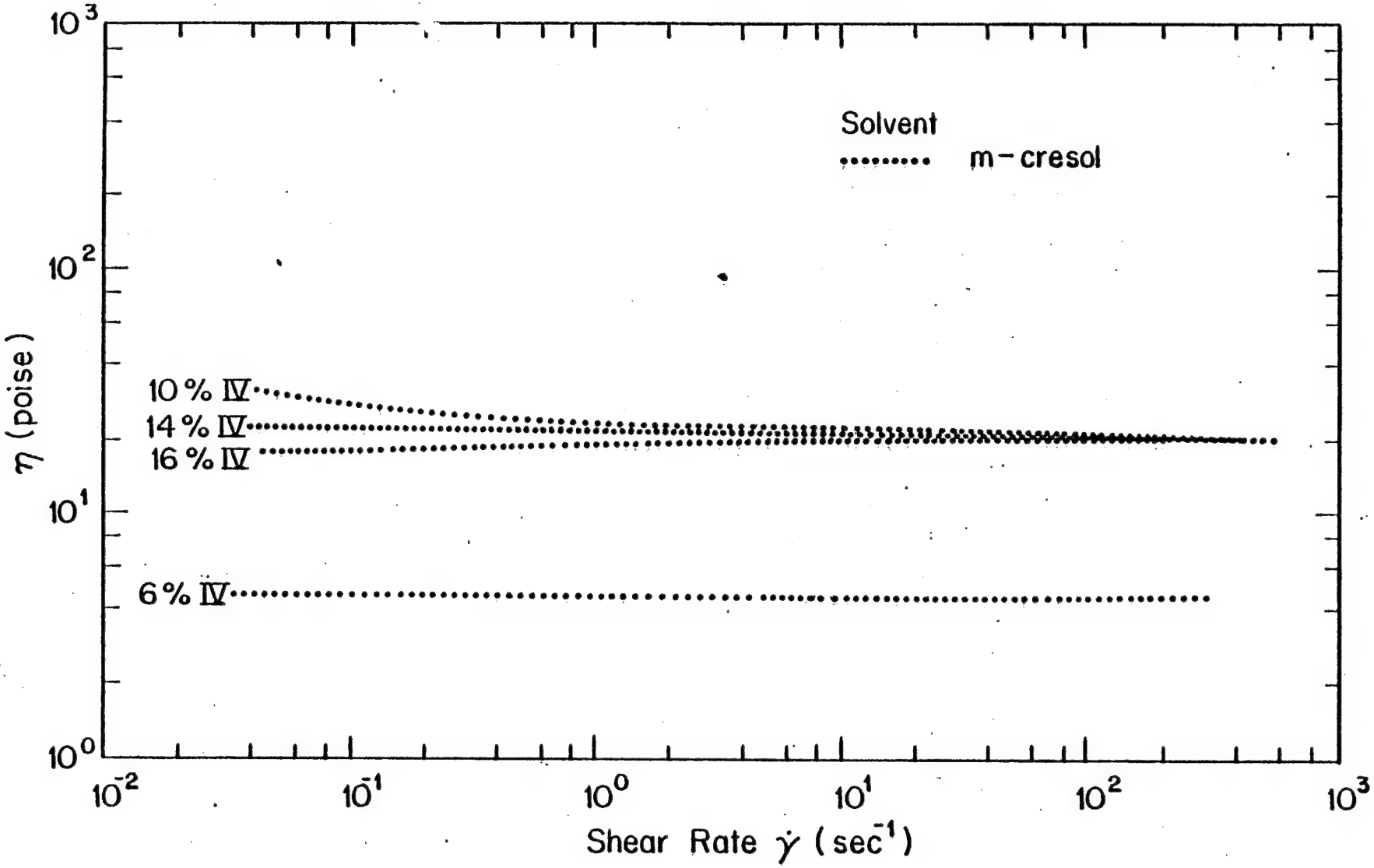

FIGURE 8. Plot of viscosity η for Kevlar® /H_2SO_4 at 25°C as a function of shear stress σ_{12}.

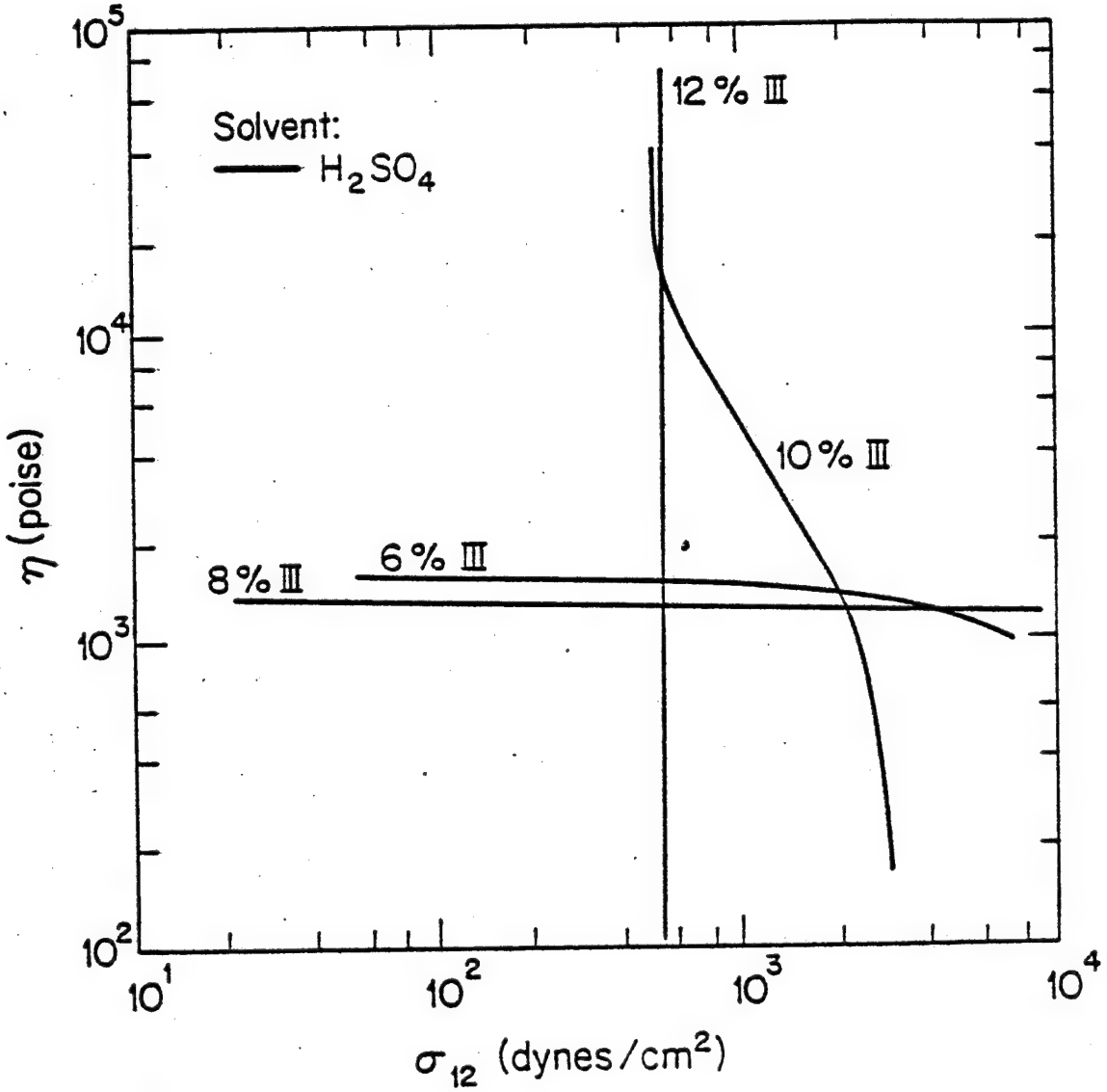

FIGURE 9. Viscosity as a function of concentration for Kevlar® /H_2SO_4 at 25°C (0.1 and 4.0 SEC^{-1}), Kevlar® /H_2SO_4 at 60°C, PγBLG/m-cresol and Nomex® /H_2SO_4 at 25°C.

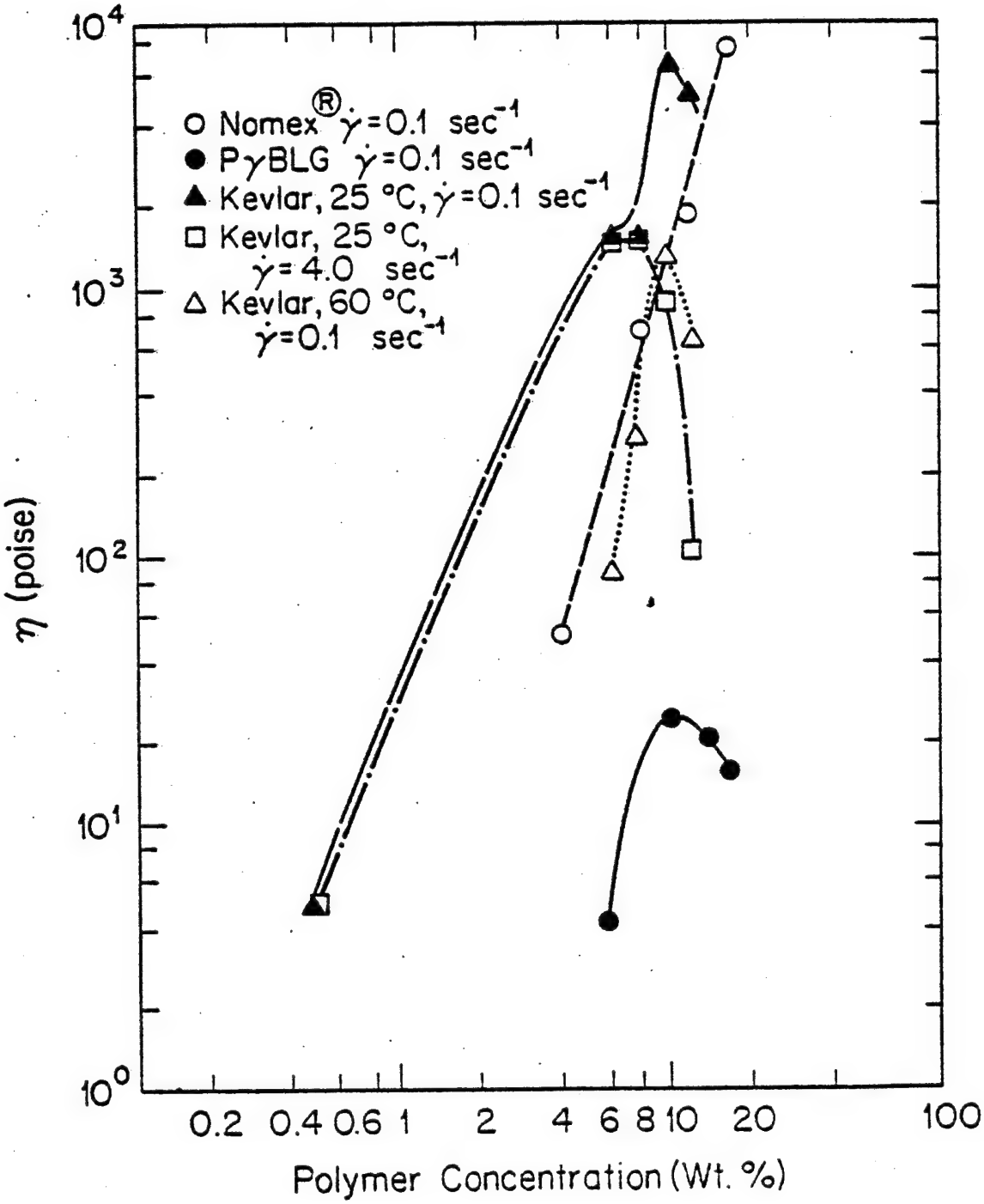

FIGURE 10. Principal normal stress difference coefficient $\psi_1(\dot{\gamma})$ as a function of shear rate and concentration for Nylon-66 in H_2SO_4 and HCOOH/10% H_2O at 25°C.

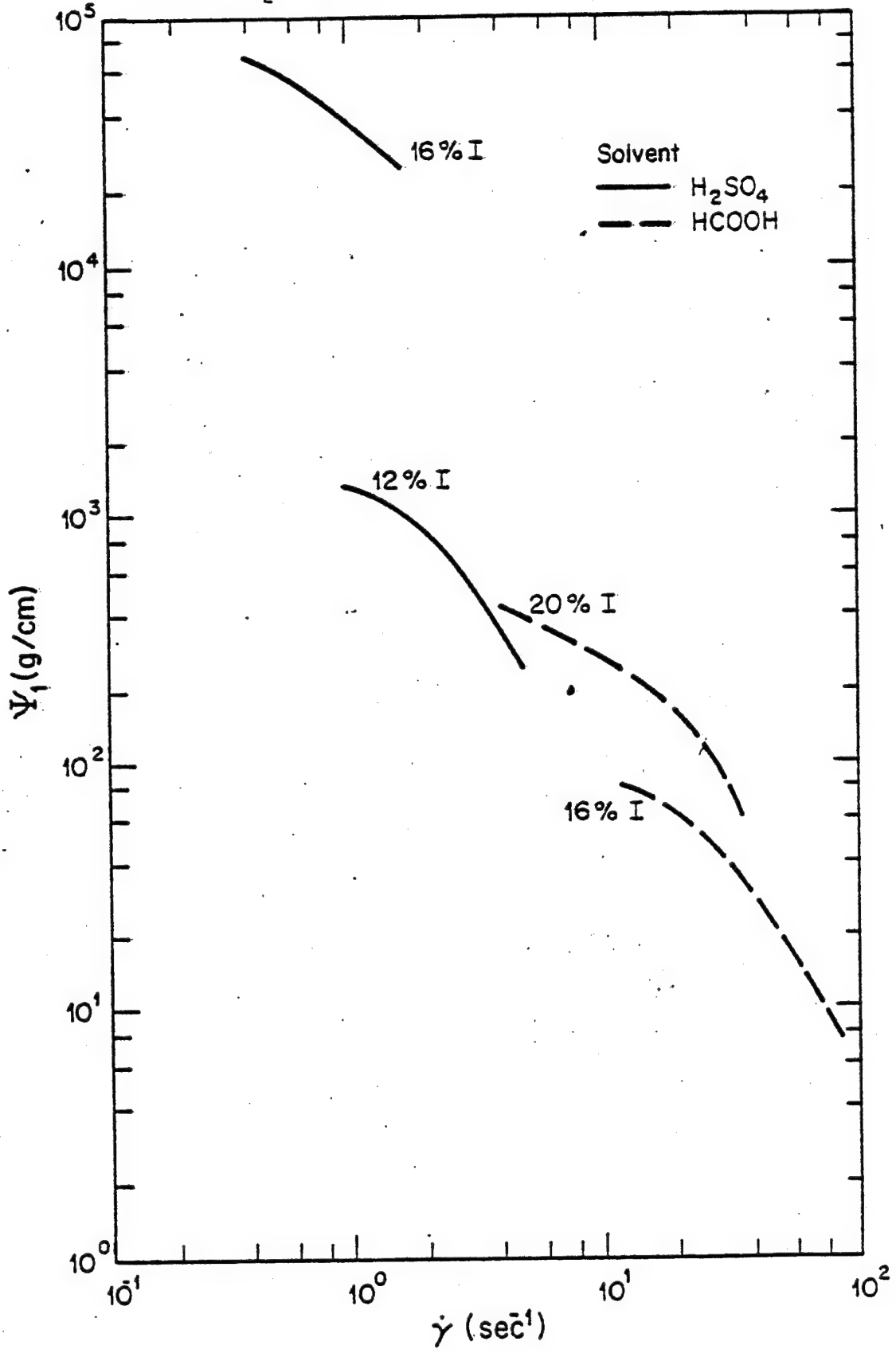

FIGURE 11. Principal normal stress difference coefficient $\psi_1(\dot{\gamma})$ as a function shear rate and concentration for Nomex® in H_2SO_4 and DMA/5% LiCl at 25°C.

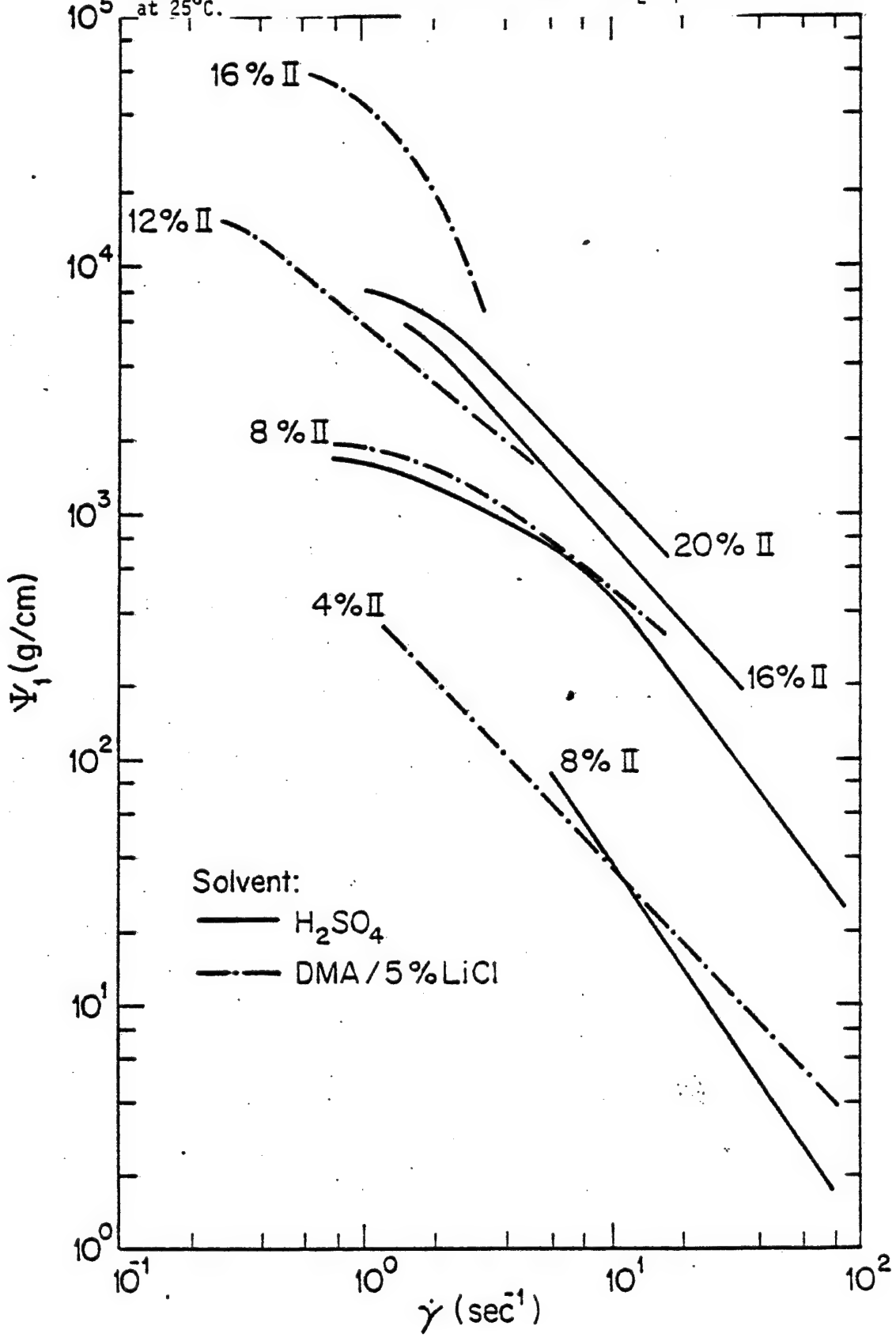

FIGURE 12. Principal normal stress difference coefficient $\psi_1(\dot{\gamma})$ as a function of shear rate and concentration for Kevlar® /H_2SO_4 solutions at 25°C.

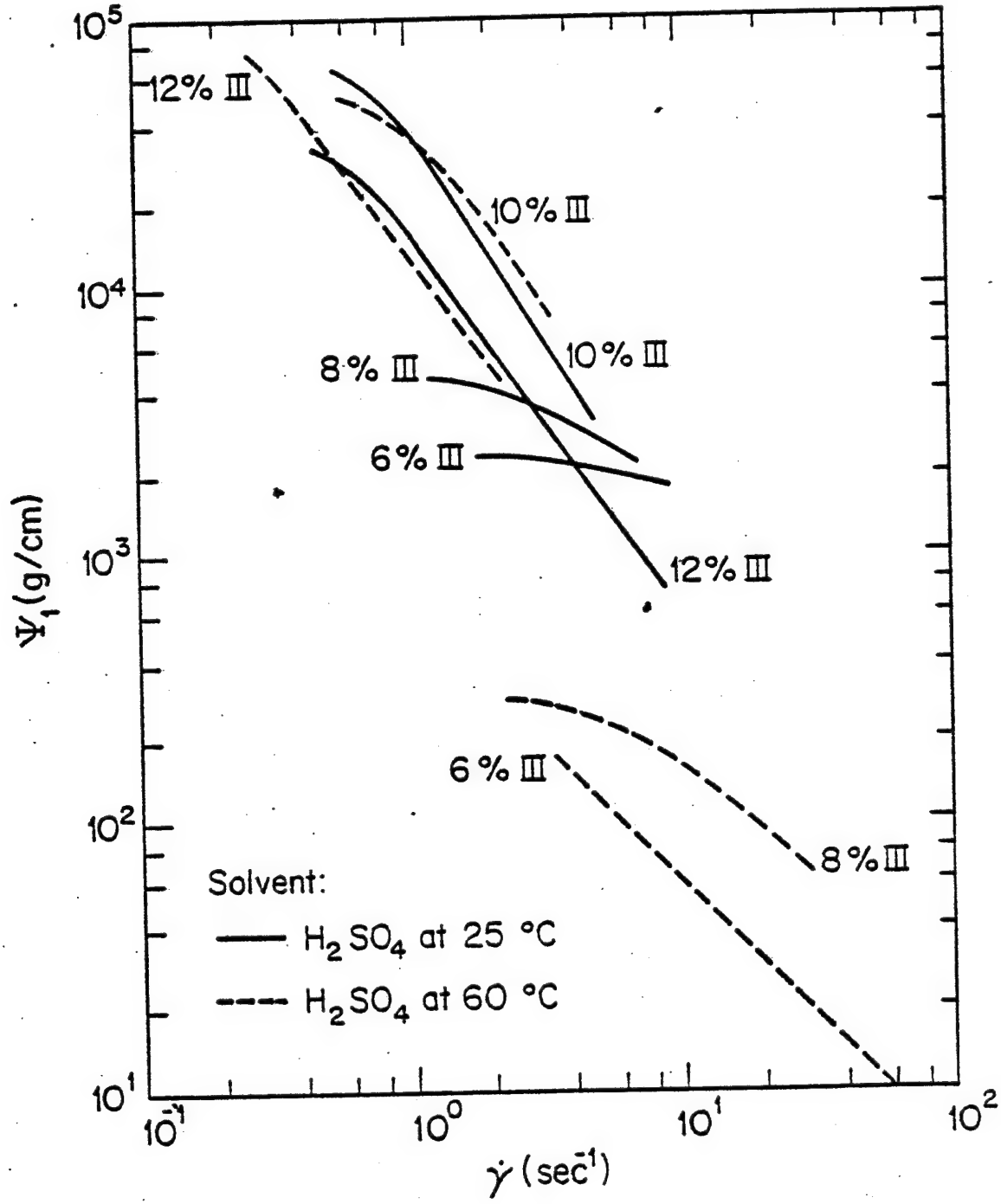

FIGURE 13. Principal normal stress difference coefficient $\Psi_1(\dot{\gamma})$ as a function of shear rate and concentration for PγBLG in m-cresol at 25°C.

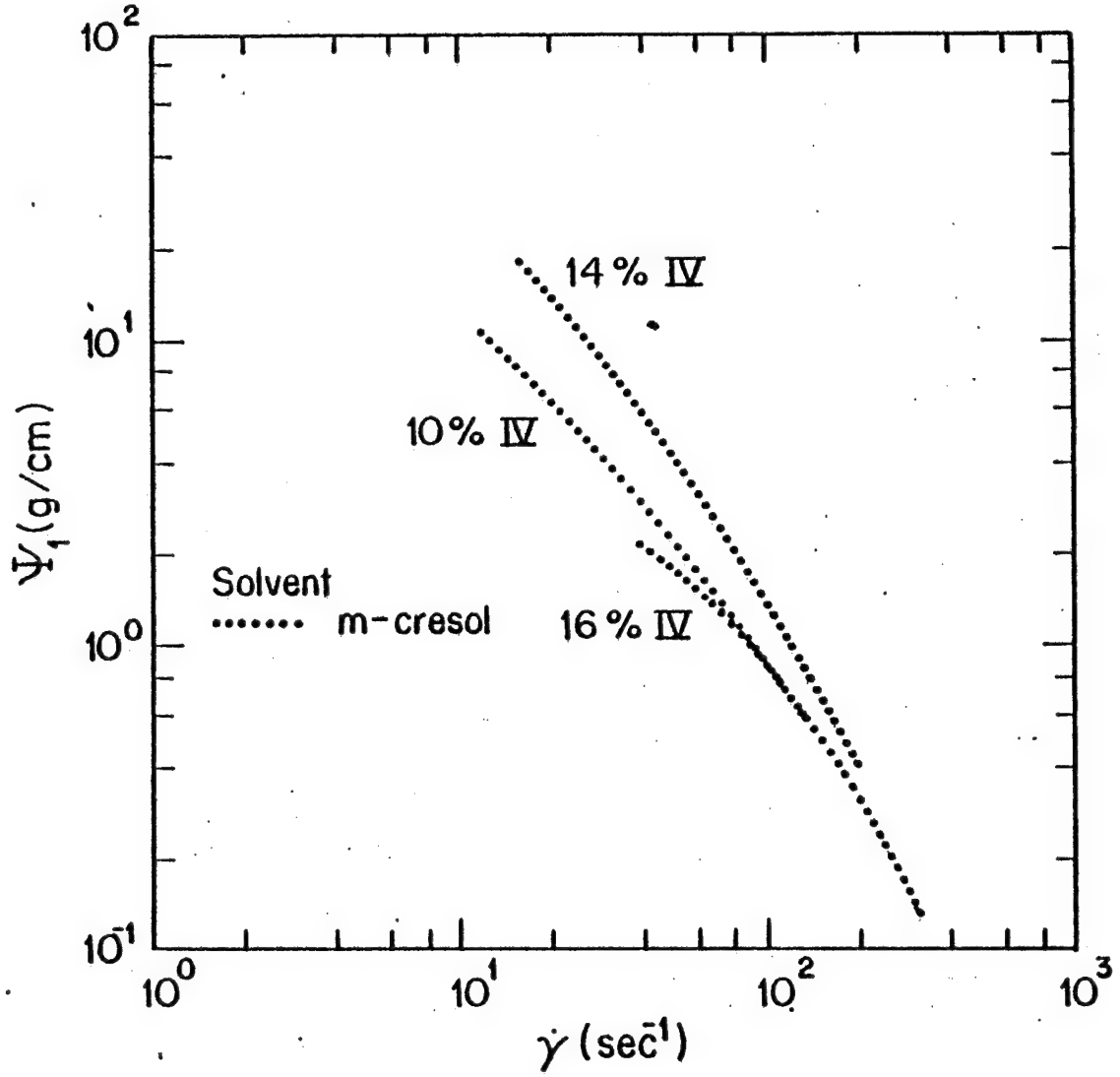

FIGURE 14. Principal normal stress difference coefficient plotted as a function of shear stress σ_{12} for Kevlar®/H_2SO_4 solutions at 25°C.

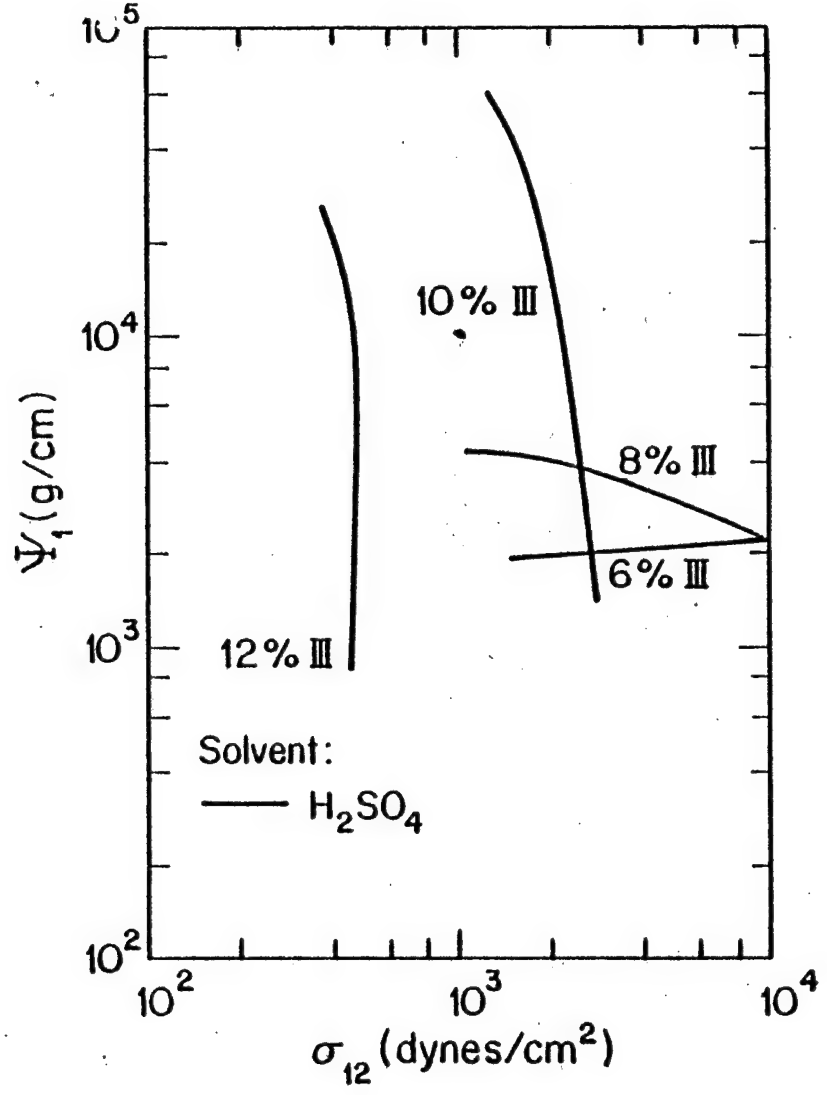

FIGURE 15. Principal normal stress difference coefficient as a function of concentration for 25°C and 60°C Kevlar® /H_2SO_4 solutions.

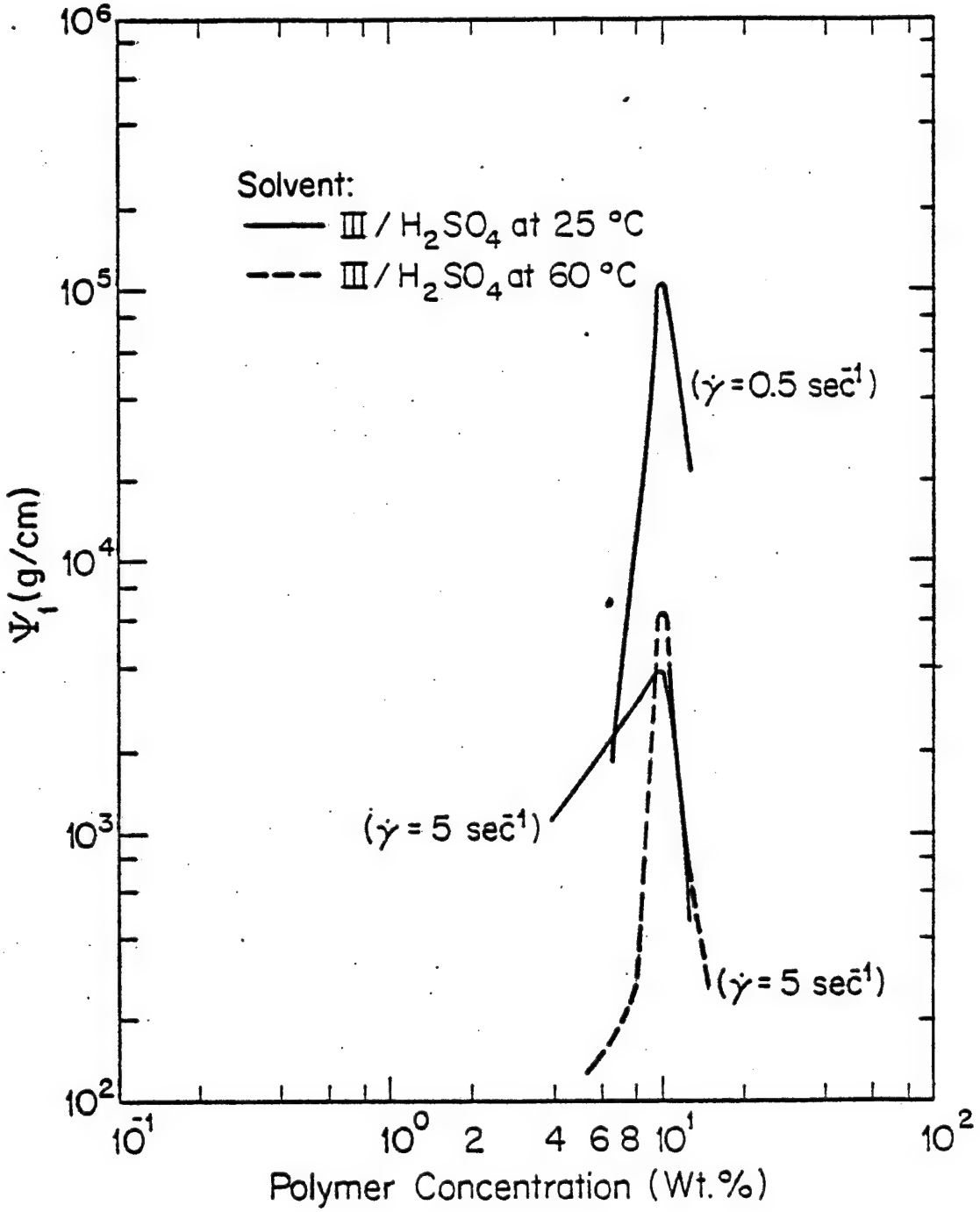

FIGURE 16a. $G'(\omega)_o$ as a function of frequency for Nylon-66 solutions in HCOOH/10%H_2O at 25°C.

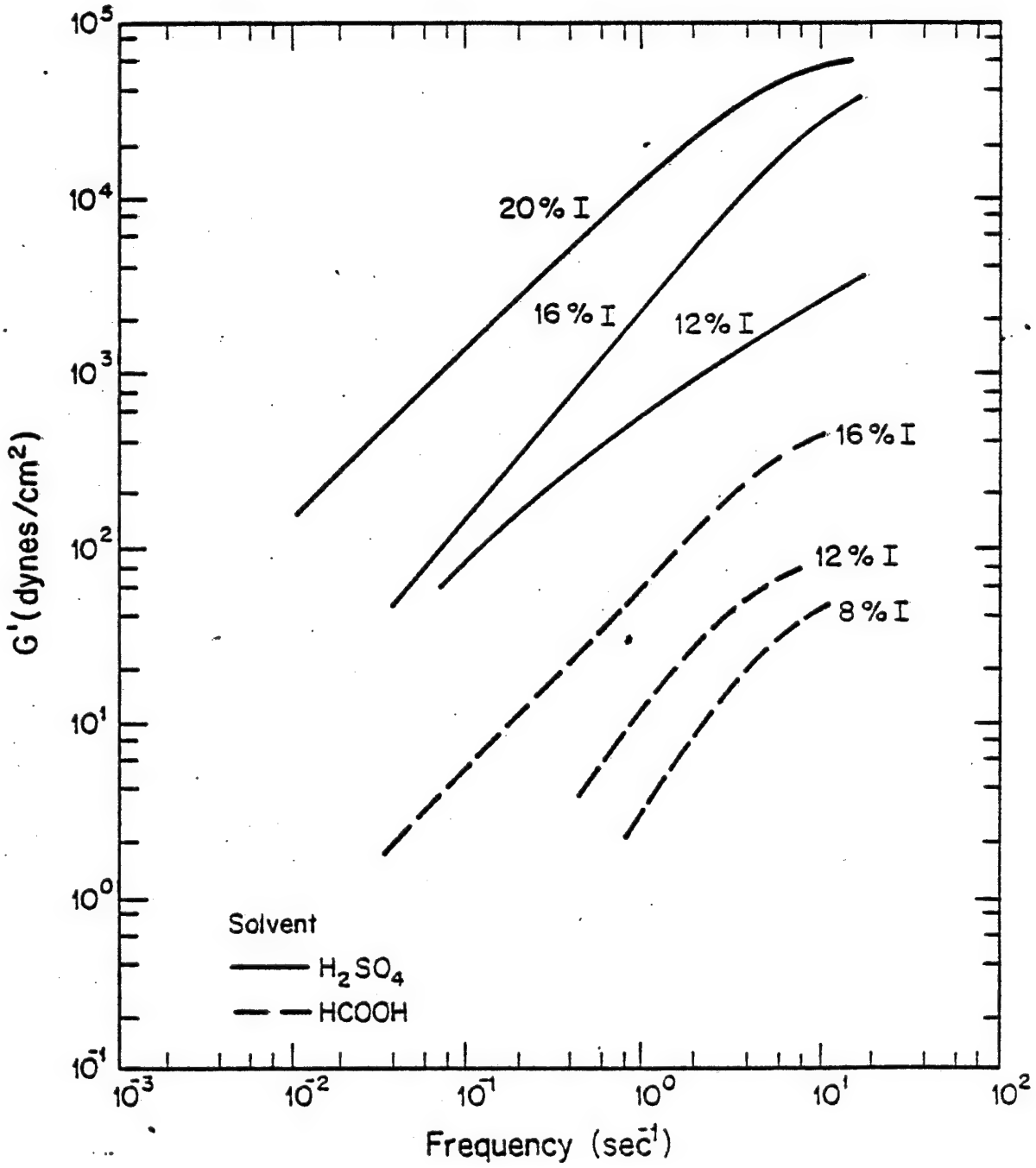

FIGURE 16b. $\eta'(\omega)$ as a function of frequency for Nylon-66 solutions in HCOOH/10%H_2O at 25°C.

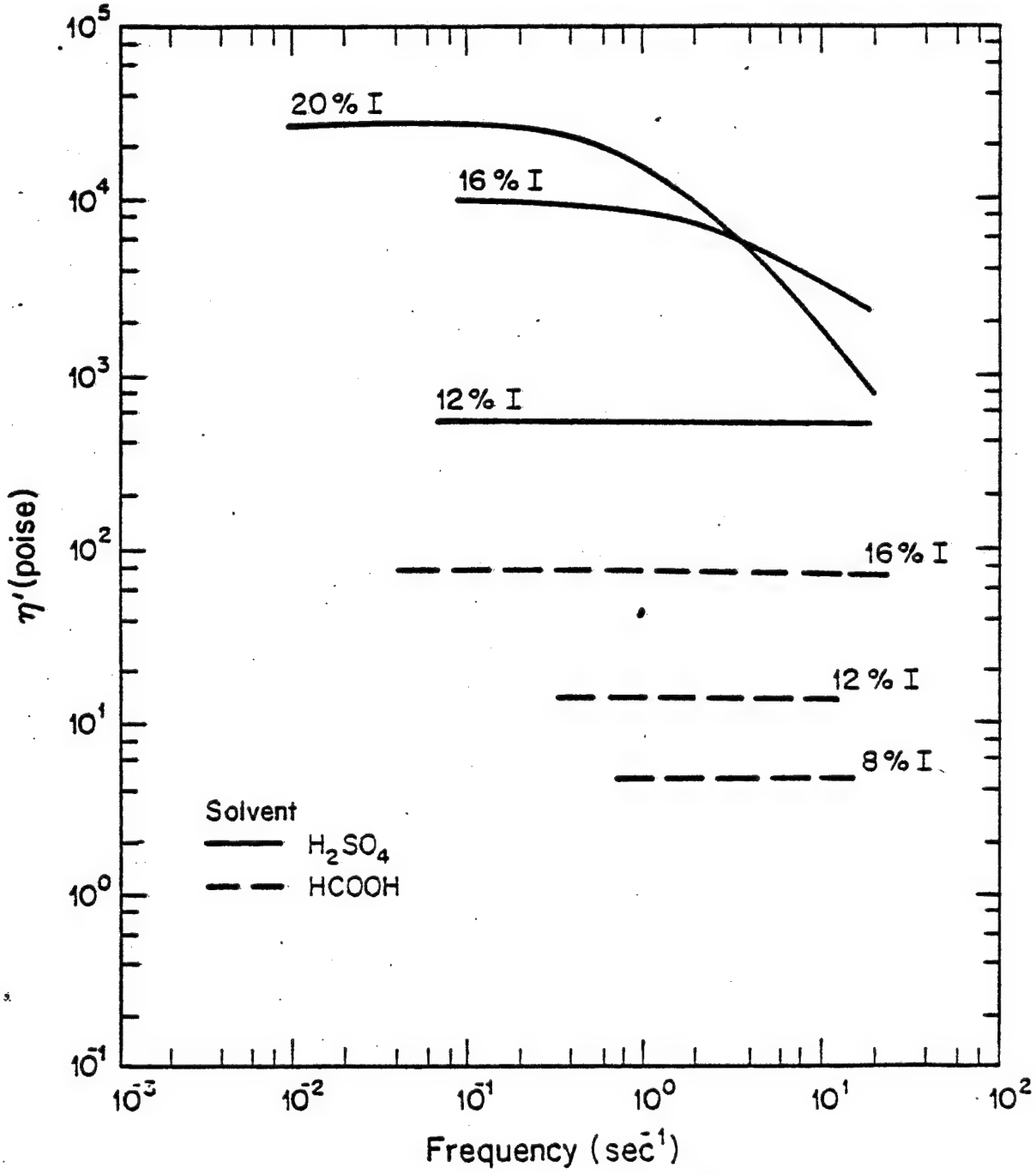

FIGURE 17a. G'(ω) as a function of frequency for Nomex® solutions at 25°C.

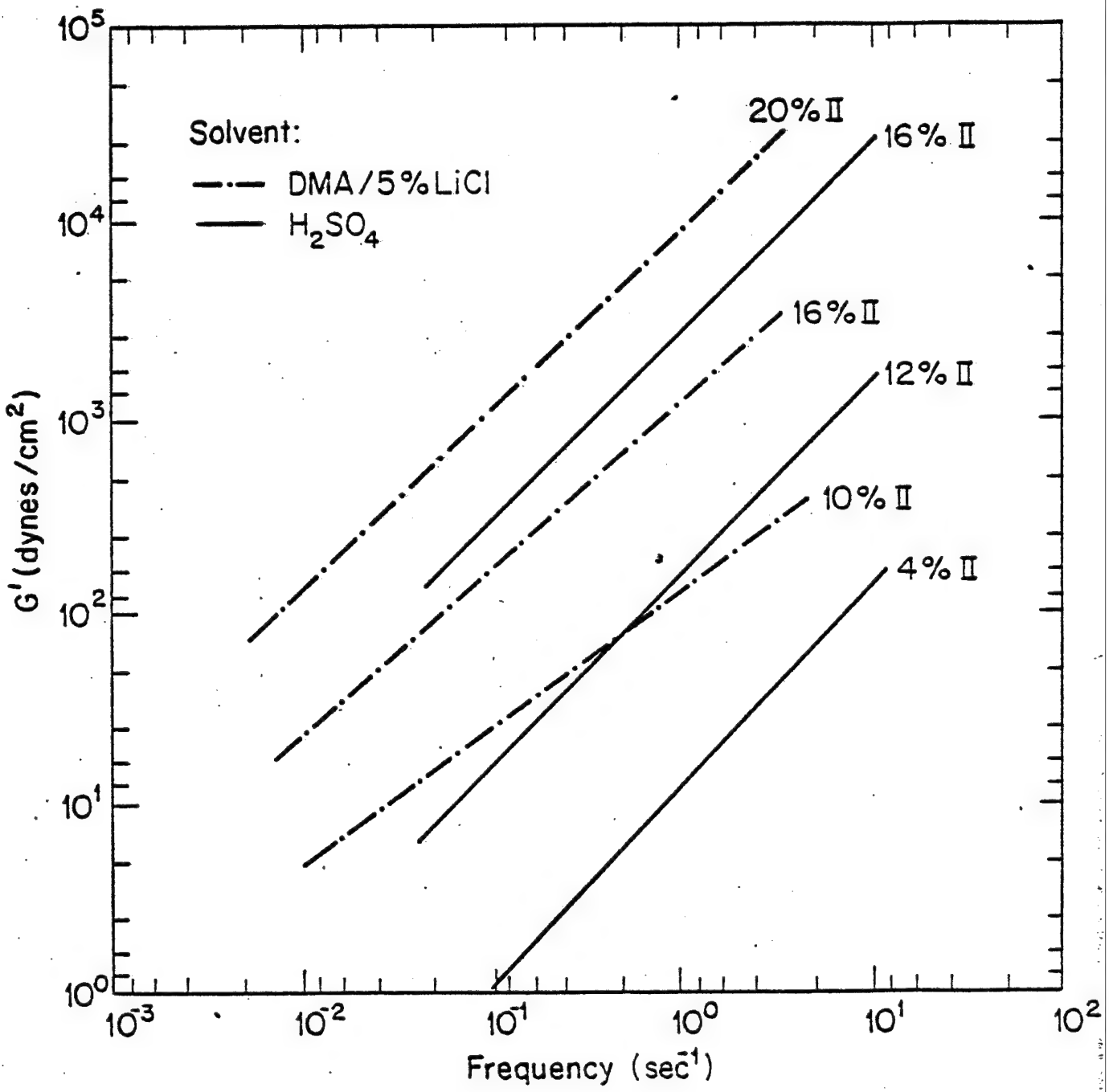

FIGURE 17b. $\eta'(\omega)$ as a function of frequency for Nomex® solutions at 25°C.

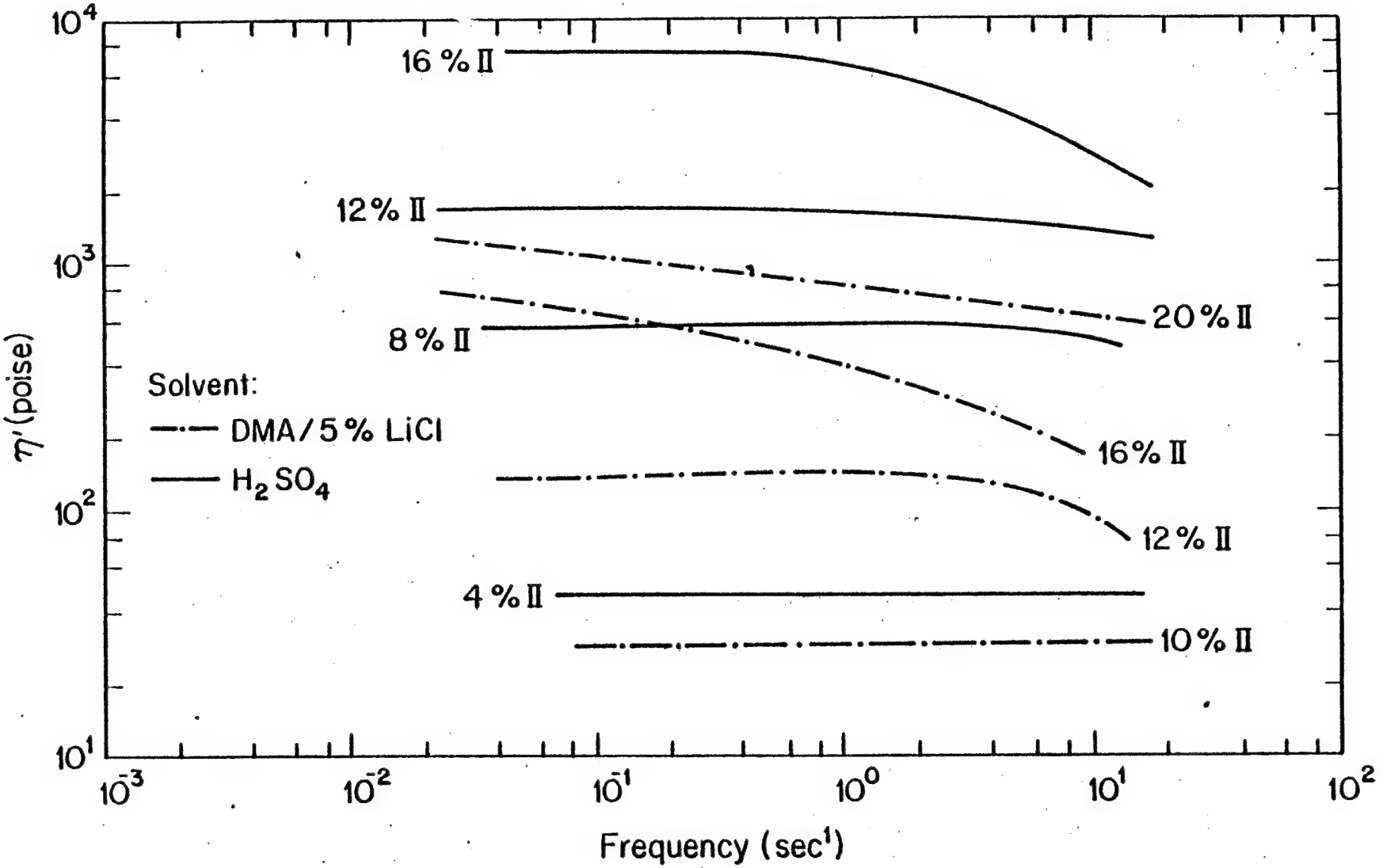

FIGURE 18a. $G'(\omega)$ as a function of frequency for Kevlar® in H_2SO_4 at 25°C and 60°C.

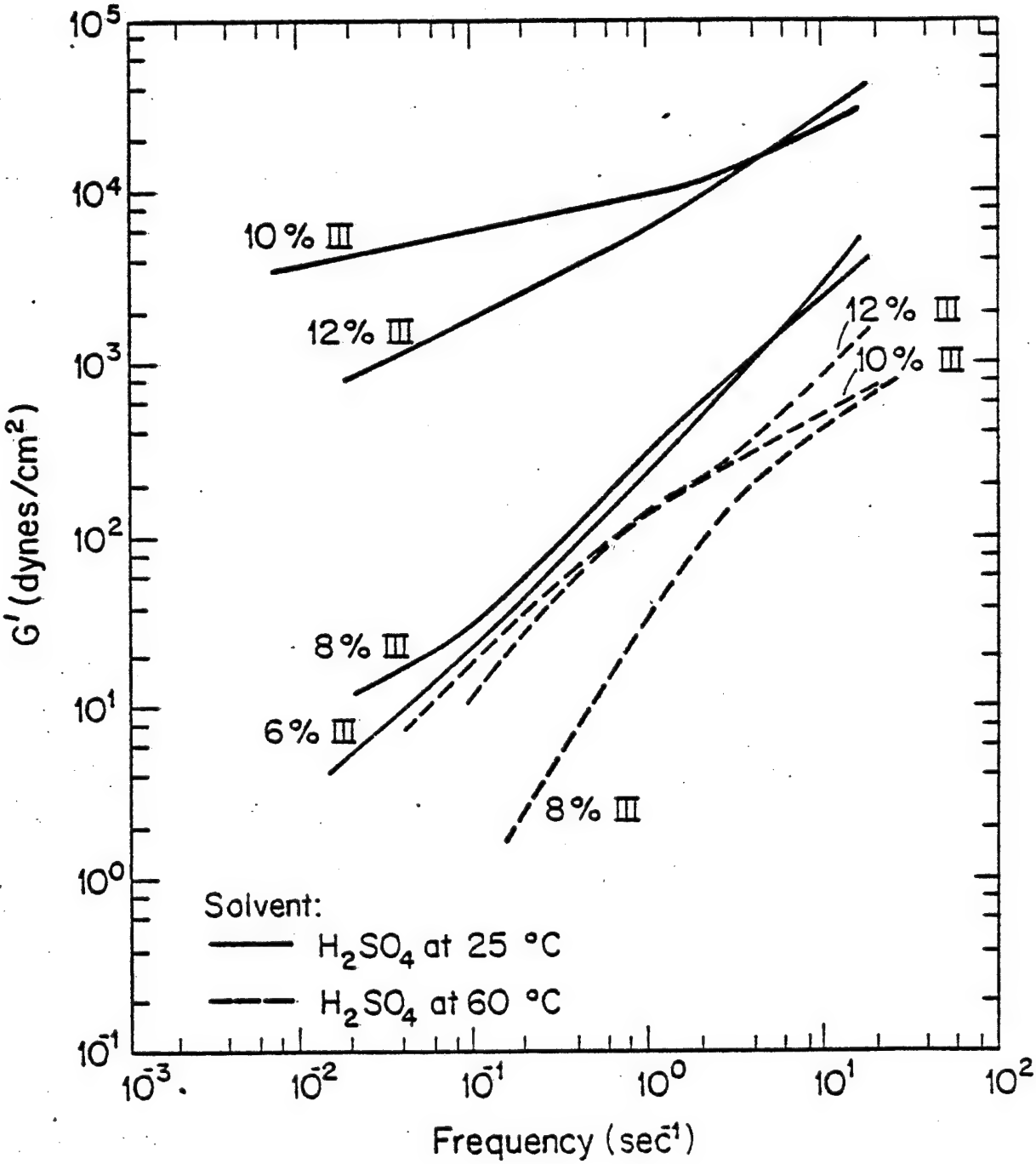

FIGURE 18b. $\eta'(\omega)$ as a function of frequency for Kevlar® in H_2SO_4 at 25°C and 60°C.

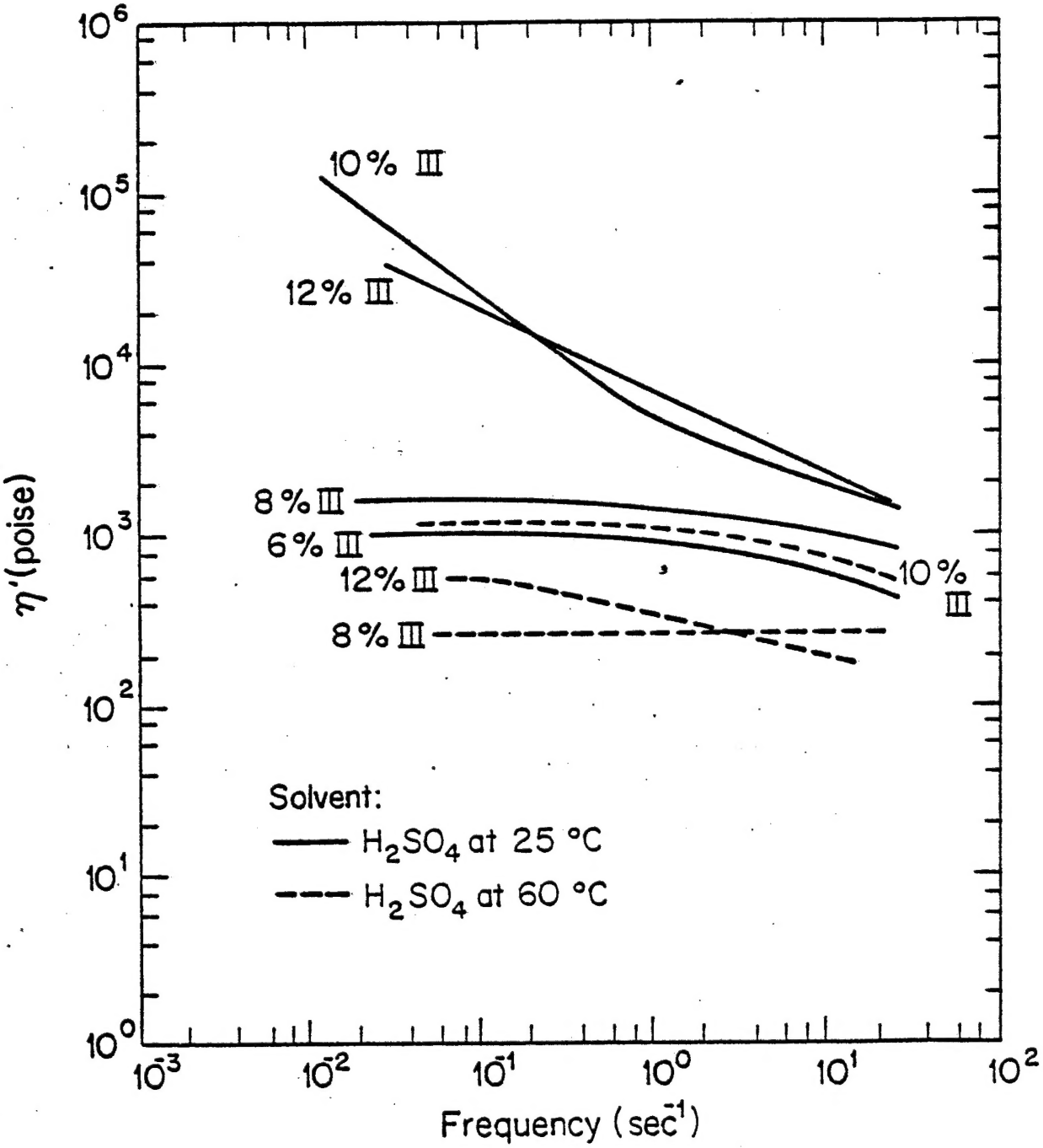

FIGURE 19. Length of threads to break for the Nylon-66 in H_2SO_4 and HCOOH spinnability experiments as a function of moving member speed and concentration at 25°C.

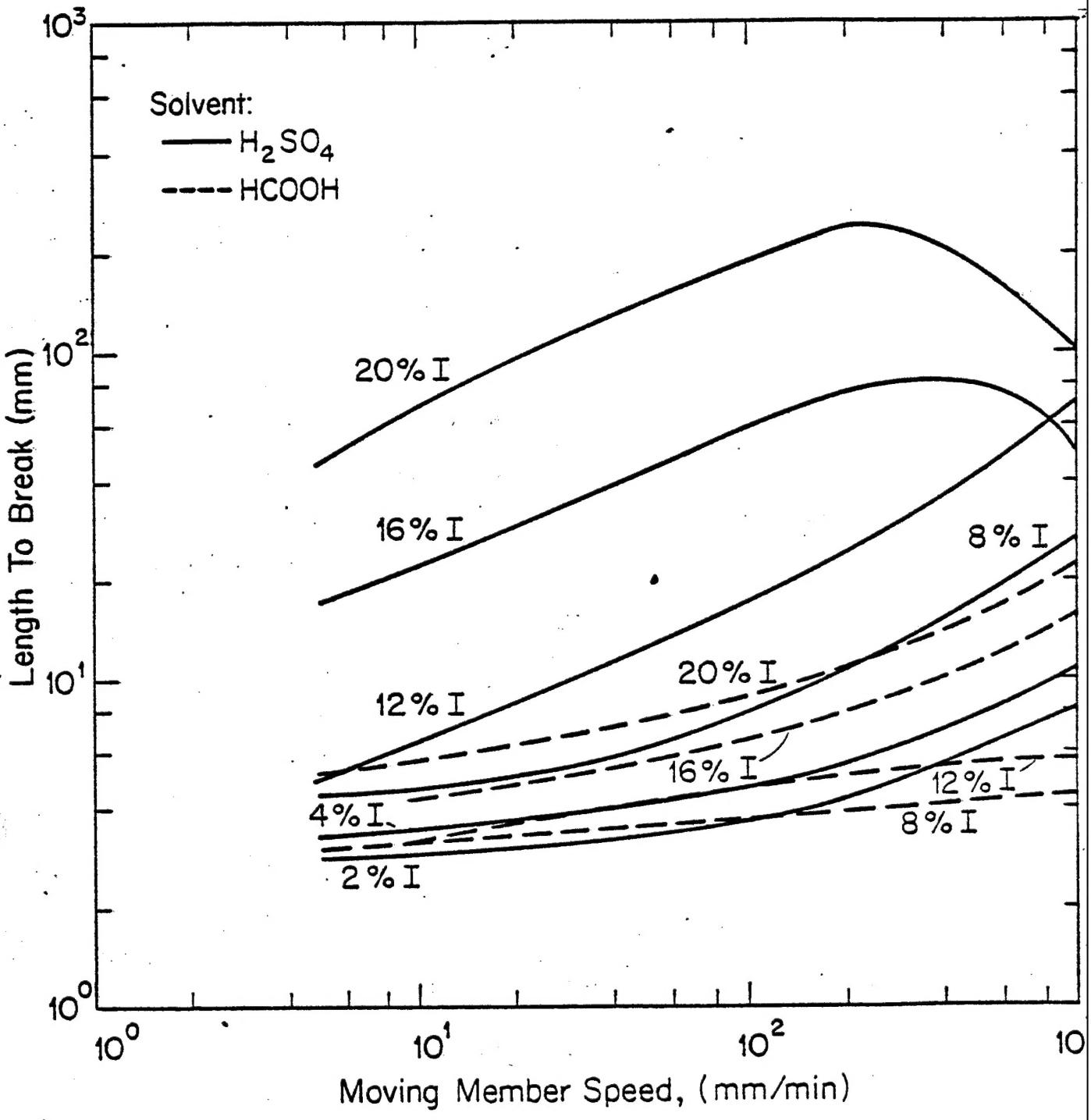

FIGURE 20. Length of threads to break for the Kevlar® /H_2SO_4 as a function of moving member speed and concentration at 25°C.

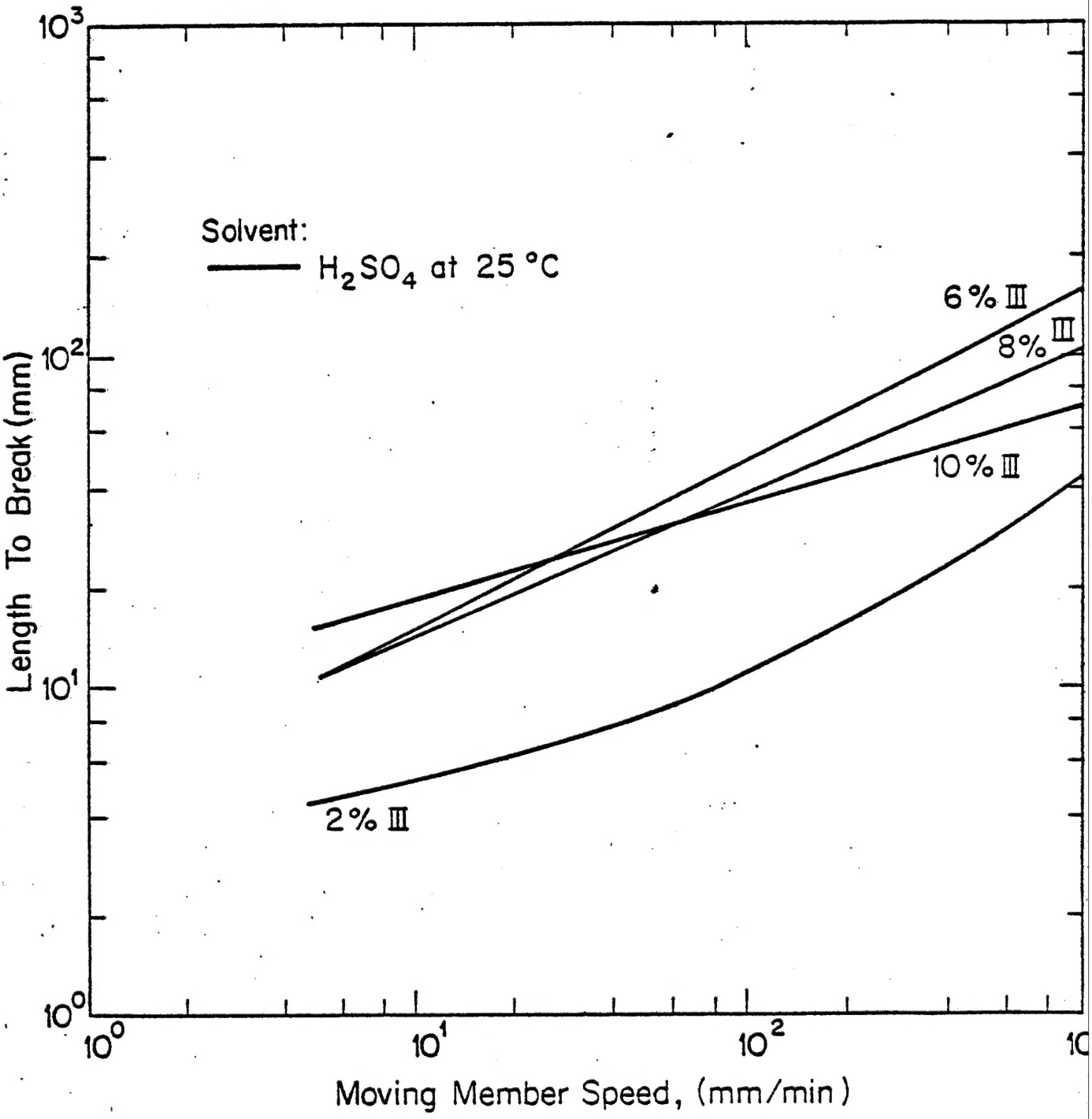

FIGURE 21. Comparison of length to break for Nylon-66, Nomex® and Kevlar® 8% solutions.